ChemComm

RSC Publishing

FEATURE ARTICLE

View Article Online
View Journal | View Issue

Cite this: *Chem. Commun.*, 2013, **49**, 429

Advances in modifying fluorescein and rhodamine fluorophores as fluorescent chemosensors

Hong Zheng,*[a] Xin-Qi Zhan,[b] Qing-Na Bian[a] and Xiao-Juan Zhang[a]

Received 18th August 2012,
Accepted 24th October 2012

DOI: 10.1039/c2cc35997a

www.rsc.org/chemcomm

The fluorophores based on xanthene scaffolds, mainly containing rhodamine and fluorescein dyes, have attracted considerable interest from chemists due to their excellent photophysical properties such as high absorption coefficient, high fluorescence quantum yield, high photostability and relatively long wavelengths of fluorescence emission spectra. In this feature article, we overview the strategies in the development of fluorescent probes that are operating through the modification of the skeletons of fluorescein and rhodamine dyes, and the fluorescent behaviors of these probes toward specific analyte are discussed.

Introduction

Fluorescent probes offer considerable advantages such as high sensitivity and specificity and versatile measurement parameters (excitation and emission spectra, intensities, intensity ratio, lifetimes or anisotropy). Combined with imaging techniques, fluorescent probes are capable of sensing and visualizing the analytes in living cells microscopically, and even in whole living animal bodies because light can travel through and emerge from biological environments. With the development of related scientific research, more fluorescent probes with higher performance are demanded, and thus the design, development, and application of novel fluorescent probes continue to be topics of a vibrant and highly multidisciplinary research area.

Among the numerous classes of highly fluorescent dyes, the sets based on xanthene scaffolds mainly containing rhodamine and fluorescein dyes (Scheme 1) have attracted considerable interest from chemists due to their excellent photophysical properties such as high absorption coefficient, high fluorescence quantum yield, high photostability and relatively long

[a] *Department of Chemistry, College of Chemistry and Chemical Engineering, and the MOE Key Laboratory of Analytical Sciences, Xiamen University, Xiamen 361005, China*
[b] *Department of Basic Medicine Science, Medical College of Xiamen University, Xiamen 361005, China. E-mail: hzheng@xmu.edu.cn; Fax: +86 592 2186731*

Hong Zheng

Dr Hong Zheng received his BS in Chemistry from Xiamen University in 1988. *He then further received his MS in Organic Chemistry in* 1995 *and PhD in Analytical Chemistry in* 1999 *from Xiamen University under the supervision of Professor Pei-Qiang Huang and Jin-Gou Xu, respectively. In* 2003, *he moved to the Department of Chemistry of Xiamen University as an associate professor after completing two years of postdoctoral research at College of Ocean and Earth Sciences from the same university. His research interests are functional organic molecules, mainly in the synthesis of long wavelength fluorescent dyes as chemosensors.*

Xin-Qi Zhan

Dr Xin-Qi Zhan received her BS in Chemistry from Xiamen University in 1988. *She then taught chemistry in the Department of Chemistry of Zhangzhou Normal University (*1988–2004*) and during the time she received her MS in Environmental Science from Xiamen University in* 2001. *In* 2010, *she received her PhD in Analytical Chemistry from the same university under the supervision of Professor Jin-Gou Xu. She is currently an associate professor at Medical College of Xiamen University. Her research interests are mainly in the area of biomedical molecular spectroscopy.*

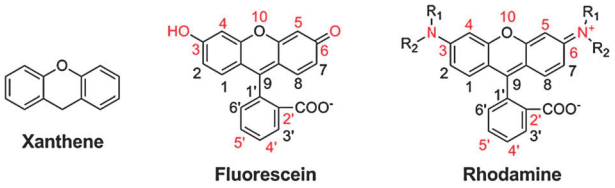

Scheme 1 The general structure of xanthene, fluorescein and rhodamine and the possible sites for modification (in red).

emission wavelength. Originally prepared by Noelting and Dziewonsky in 1905 and von Bayer in 1871, respectively,[1,2] rhodamine and fluorescein derivatives have been widely and successfully applied in many fields including biology and medicine. Although bearing a history of more than one hundred years, they nowadays still retain their strong vitality. Since there are many possible reactive sites in the skeleton of fluorescein or rhodamine for organic modification (mainly including positions 4 and/or 5, 3 and/or 6, 10, 2′, 4′ and/or 5′, and the hydroxyl and amino groups, see Scheme 1), numerous derivatives of rhodamine and fluorescein dyes have been reported using synthetic strategies in recent years to satisfy various practical demands, especially for designing chemosensors. For example, a derivatisation reaction of a carboxylic acid group at position 2′ to form its secondary amide of rhodamine dyes, usually present in non-fluorescent spirolactam, as molecular sensors, has gained its remarkable progress since 2000, in which an appropriate ligand on the spirolactam ring can induce color change as well as fluorescence enhancement in the presence of analyst species by opening the spiro-ring (Scheme 2).

Except those of spiro-lactam based probes, chemical modifications of other sites in the skeletons of rhodamine and/or fluorescein dyes also have strong influence on their fluorescent behavior, which can be utilized to design chemosensors. In this feature article, we put our focus on the selected examples of chemosensors for small target analytes in recent years, which are categorized by the modification strategies on the sites in rhodamine and fluorescein fluorophores' skeletons, and their application is also included. Therefore, six types of position-related modifications in fluorescein/rhodamine fluorophores enabling us to design molecular chemosensors can be included: (i) modification of the hydroxyl or amino groups on the ring of xanthene moieties, (ii) chemosensors derived from the xanthene ring at positions 4 and/or 5, (iii) chemosensors derived from the xanthene ring at positions 3 and/or 6, (iv) chemosensors derived from derivatisation reactions at position 2′, and as regards to this item, those namely spirolactam-based chemosensors in Scheme 2, which have recently gained broad attention in excellent review articles,[3–8] were thus excluded. However, the probes of modifications at position 2′ to afford other spiro-ring systems of rhodamine scaffolds would be included, because in view of organic chemistry, these compounds could not be ascribed to spiro-lactam species, (v) replacement of the bridging oxygen atom in the xanthene ring at position 10, and the last, (vi) chemosensors derived from the phenyl ring at positions 4′ and/or 5′. We hope that the discussion of these chemosensors would help to catch the highlights in the development of chemosensors and thus broaden the designing methodologies in this field.

Scheme 2 Spiro-lactam ring-opening of rhodamine secondary amide derivative.

Modification of the hydroxyl or amino group on the ring of xanthene moiety

It is usually that functionalization of the hydroxyl or amino groups of xanthene moieties of fluorescein and rhodamine dyes can lead to severe changes in their photophysical properties, and/or transfer to spirolactone conformation, causing the loss of fluorescence to some extent, as a result, this property was found useful for the synthesis of latent fluorophores.

By fusing the phenolic hydroxy group of a fluorescein fluorophore in a 4-amino- or a 4-hydroxylphenyl ether moiety,

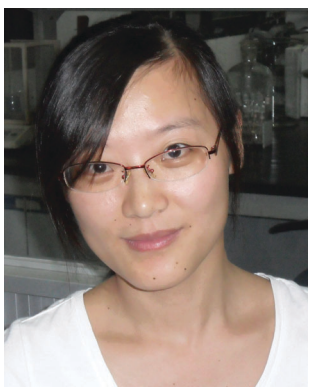

Qing-Na Bian

Qing-Na Bian was born in Shandong, China, in 1988. She received her BS in Chemistry from Shandong Normal University in 2010. She is currently pursuing her MS study at the Department of Chemistry, Xiamen University, under the supervision of Dr Hong Zheng. Her research interests mainly focused on the development of fluorescent probes for some analytes of biological interest and their applications in physiological system.

Xiao-Juan Zhang

Xiao-Juan Zhang received her BS in Applied Chemical from Anhui University in 2010. She is currently pursuing her MS study at the Department of Chemistry, Xiamen University, under the supervision of Dr Hong Zheng. Her research interests include the synthesis of fluorescent chemosensors and investigating of their applications in recognition ions and neutral molecules.

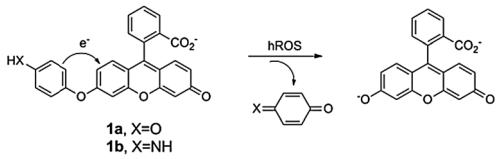

Fig. 1 Sensing of hROS through an oxidative O-dearylation reaction.

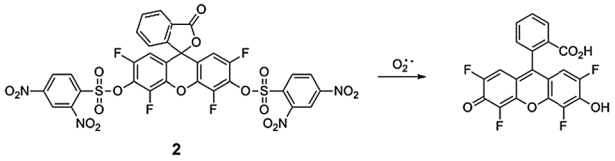

Fig. 2 Sensing of $O_2^{\bullet-}$ by the cleavage of the benzenesulfonate bonds.

which is more electron-rich than the xanthene moiety that could be used to quench the fluorescence of fluorescein through photoinduced electron transfer (PET), Nagano's group designed and synthesized two novel fluorescein-based probes, **1a** and **1b**,[9] as highly reactive oxygen species (hROS) sensors (Fig. 1). These almost nonfluorescent probes could be O-dearylated upon reaction with hROS to yield strongly fluorescent products of fluorescein, and they showed fluorescence augmentation only upon reaction with $^{\bullet}OH$, $ONOO^-$, and/or ^-OCl, and not with $O_2^{\bullet-}$, H_2O_2, $^1O_2$, NO, and $ROO^{\bullet}$.

Maeda and co-workers developed a highly specific fluorescent probe, **2**, for detection of $O_2^{\bullet-}$ in a turn-on mode of fluorescence,[10] which is based on a non-redox mechanism (Fig. 2). The probe, engineered with two 2,4-dinitrobenzenesulfonyl groups (DBS) as protection groups and predominated the spirolactone conformation, provided a highly sensitive method for measuring $O_2^{\bullet-}$ generated in the enzymatic xanthine oxidase (XO)/hypoxanthine (HPX) system at 37 °C or KO_2 in DMSO-HEPES buffer at room temperature, which subsequently underwent a cleavage of the benzenesulfonate bonds to afford the ring-opening product with strong fluorescence. A detection limit of 1.0 pmol per well was obtained. The proposed chemosensor has been used for direct measurement of cell-derived $O_2^{\bullet-}$ using neutrophils stimulated with phorbol myristate acetate.

Tang and co-workers described the chemical synthesis, property analysis and biological application of the diphenylphosphinate fluorescein (**3**), a new type of phosphinate-based fluorescent probe for imaging $O_2^{\bullet-}$ in biological environments (Fig. 3).[11] The design strategy for the probe was based on the nucleophilic properties of

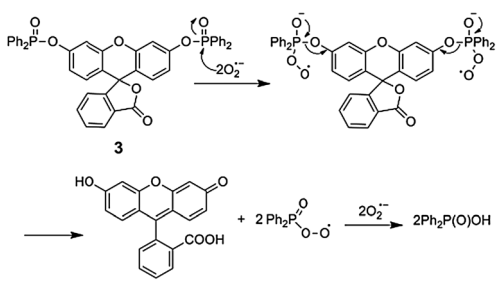

Fig. 3 Sensing of $O_2^{\bullet-}$ by the nucleophilic properties of $O_2^{\bullet-}$.

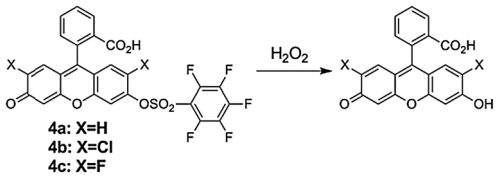

Fig. 4 Sensing of H_2O_2 by pentafluorobenzenesulfonyl fluoresceins **4**.

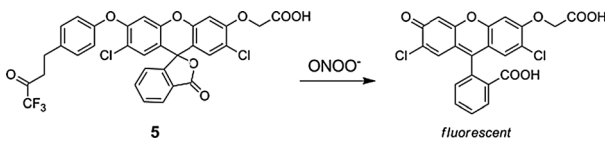

Fig. 5 Sensing of $ONOO^-$ by a tandem $ONOO^-$ induced dioxirane-oxidative reaction.

$O_2^{\bullet-}$. The probe mediates deprotection of a diphenylphosphinate moiety, leading to ring-opening of spirolactone fluorescein. In aqueous solution (pH = 7.4), **3** displays an excellent selectivity toward $O_2^{\bullet-}$ over other ROS (reactive oxygen species)/RNS (reactive nitrogen species) and biologically relevant compounds with a detection limit of 4.6 pM. Furthermore, the probe is cell-permeable and can detect micromolar changes in $O_2^{\bullet-}$ concentrations by using confocal microscopy in living cells.

Maeda and co-workers designed pentafluorobenzenesulfonyl fluoresceins (**4a–c**) as novel fluorescent probes with a non-oxidative mechanism that has a high selectivity toward H_2O_2 over $HO^{\bullet}$, *t*-BuOOH, $ONOO^-$, $O_2^{\bullet-}$, and $^1O_2$ in pH 7.4 HEPES buffer (Fig. 4).[12] These new probes can facilitate the measurements of cell-derived H_2O_2 and elucidate the dynamic functions of oxidative stress.

A peroxynitrite-selective probe, **5**, which contains a dichlorofluorescein moiety linked with a ketone unit *via* an aryl ether spacer, was reported by Yang and co-workers (Fig. 5).[13] Upon treatment with peroxynitrite *in situ,* the ketone unit of the probe generated a dioxirane that subsequently oxidized the phenyl ring to afford the strong fluorescent product. Probe **5** appears to be highly selective for peroxynitrite compared with other reactive oxygen species such as NO, $^1O_2$, $O_2^{\bullet-}$, $^{\bullet}OH$, $ROO^{\bullet}$, ClO^- and is demonstrated to detect peroxynitrite in living primary cultured neuronal cells.

Three novel water-soluble probes (**6a–c**) with a dihydrofluorescein component were designed by Yao and co-workers (Fig. 6),[14] which could selectively detect HOCl by a specific HOCl-promoted oxidation reaction resulting in a photo switch from non-fluorescent

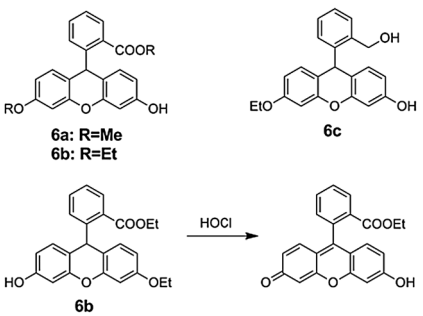

Fig. 6 Dihydrofluorescein derivatives **6** for HOCl.

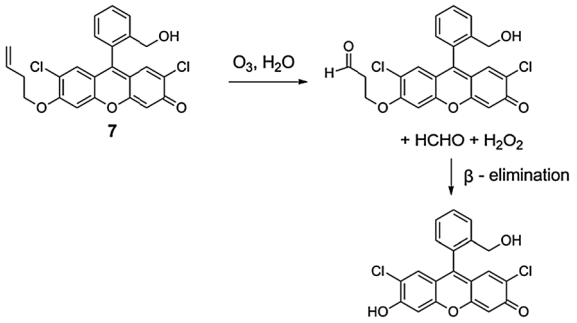

Fig. 7 Sensing of ozone by tandem ozonolysis-β-elimination reaction in **7**.

deconjugated form to strongly fluorescent conjugated form. **6b** showed fast response time (~20 min) and high selectivity toward HOCl over other biologically relevant ROS and RNS. Meanwhile, it displayed the larger fluorescence enhancement (1643.4-fold) and an extraordinarily lower detection limit (0.71 ppb). **6b** could not only visualize HOCl produced by MPO-mediated peroxidation of chloride ions in living cells, but also estimate the accumulated HOCl level in zebrafish organs.

Koide and co-workers also reported a specific and turn-on fluorescent probe **7** for ozone which was based on a tandem ozonolysis-β-elimination in **7** to release a fluorescent product (Fig. 7).[15] The probe showed high selectivity for ozone over other ROS such as hydrogen peroxide, hydroxy radical or biological anti-oxidants such as ascorbic acid, glutathione and uric acid. The probe is capable of fluoroscopic detection of ozone in biological and environmental samples in pH 7.0 buffer and MeOH as a co-solvent (95 : 5). The fluorescence intensity correlated with the concentration of ozone in the range of 50 nM–12.5 μM (2.4–600 ppb). The probe was proved to be useful for the study of ozone in environmental science and biology and has the potential to provide some insight into the role of ozone in cells.

Acetate groups were chosen by Chang and co-workers to mask the phenolic hydroxy group of fluorescein to furnish probe **8** (Fig. 8).[16] It was found that a perborate ion could

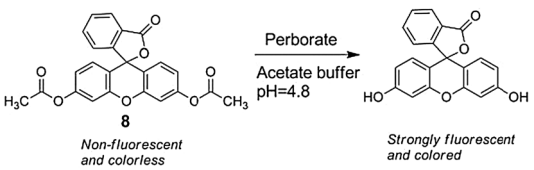

Fig. 8 Sensing of perborate by deprotecting the acetate group.

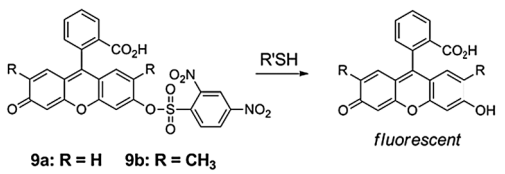

Fig. 9 Sensing of thiols by thiol-induced removal of 2,4-dinitrobenzenesulfonyl group.

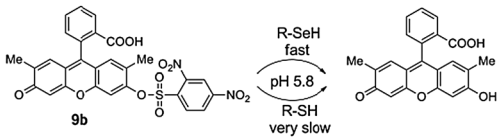

Fig. 10 Sensing of selenols by selenol-induced removal of 2,4-dinitrobenzenesulfonyl group in acidic solution.

selectively deprotect the acetate group and release the fluorophore, resulting in significant chromogenic and fluorogenic enhancement. Besides, **8** exhibited a pronounced perborate selectivity over other commonly used oxidants such as superoxide, *m*-CPBA, peracetic acid, or hydrogen peroxide in aqueous 10% acetonitrile solution (H_2O : CH_3CN = 90 : 10, v/v) at pH 4.8 with acetate buffer (10 mM).

By being monoprotected with one DBS group, almost-nonfluorescent compounds **9a** and **9b** were found to be selectively recognized towards thiols in an aqueous HEPES medium (pH 7.4), reported by the group of Maeda (Fig. 9).[17] When a thiol was added to the solution, the DBS group was efficiently removed, and compounds **9a** and **9b** were transformed effectively to highly fluorescent species with significantly shorter reaction time under mild conditions and without any side reactions. The detection limits of the two probes towards glutathione (GSH), cysteine (Cys) and $H_2NCH_2CH_2SH$ (AET) were found to be less than 2.0 pmol per well. Thus, sensors **9a** and **9b** may allow simple and reliable fluorometric systems for measuring acetyl- and butyrylcholinesterase (AChE and BChE, respectively) activities in which substrates release thiols through enzymatic reactions.

Because the pK_a value of the –SeH group in SeCys is 5.2, which is much lower than the pK_a value (8.3) of the –SH group in Cys, and because selenols behave as stronger nucleophiles than thiols, Maeda and co-workers utilized the fluorescein-derived dinitrobenzenesulfonates (**9b**) as the first fluorescent ''turn-on'' probe for selenol by merely changing the pH value of the detection medium from 7.4 to 5.8 through nucleophilic substitution of selenol (Fig. 10).[18] A selenol SeCys moiety cleaved the DBS group more than 1000-times faster than did Cys at pH 5.8 in phosphate buffer. The detection limit was 0.8 pmol per well estimated by the microtiter assay.

A novel rhodamine 6G-based fluorescent probe, **10**, containing a Se–N bond for thiols was developed by Tang and co-workers (Fig. 11).[19] The design strategy was based on the strong nucleophilicity of the sulfhydryl to cleave the Se–N bond of **10** to form the corresponding selenenyl sulfide, **11**, leading to the recovery of the strong fluorescence of rhodamine 6G. The probe exhibited high selective fluorescence response to GSH over other non-protein thiols such as 2-mercaptoethanol, *N*-acetylcysteine, Cys and dithiothreitol (DTT) under simulated physiological conditions

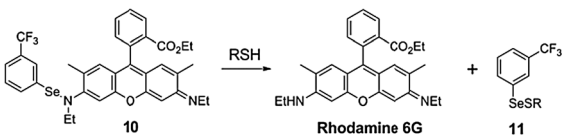

Fig. 11 Sensing of glutathione by thiol-mediated Se–N bond cleavage.

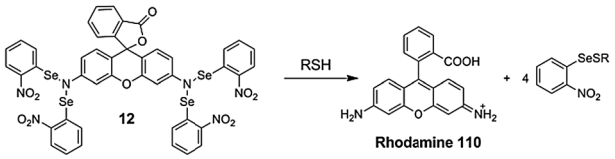

Fig. 12 Multi Se–N groups in glutathione probe **12**.

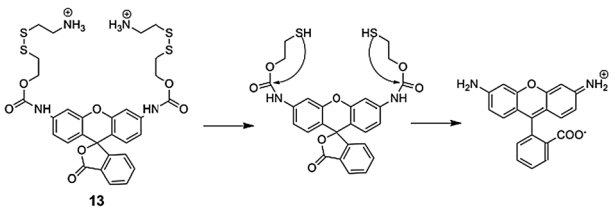

Fig. 13 Sensing of thiols by disulfide exchange.

(pH 7.4, 20 mM phosphate buffered saline). In addition, the detection limit of the probe to GSH could be down to 1.4 nM. Furthermore, the new probe was successfully applied to the imaging of thiols in both HL-7702 cells and HepG2 cells with high sensitivity and selectivity.

The same group further designed a probe (**12**) by substituting the four hydrogen atoms on the amino groups of rhodamine 110 with four Se containing groups to achieve further reduction in intrinsic fluorescence (Fig. 12).[20] Upon addition of GSH, **12** showed a higher signal-to-noise ratio (up to 170-fold) with a detection limit of 144 pM.

Chmielewski and co-workers developed a new disulfide-based fluorescent probe (**13**) which is a latent rhodamine (Fig. 13).[21] In the presence of GSH, the probe underwent a reduction reaction of the disulfide bonds, which released the nucleophilic sulfhydryl groups and caused the breakdown of the neighboring carbamate bonds, leading to the unmasking of rhodamine 110 (Rh110). **13** was also successfully applied to confocal microscopy images of GSH in live HeLa cells.

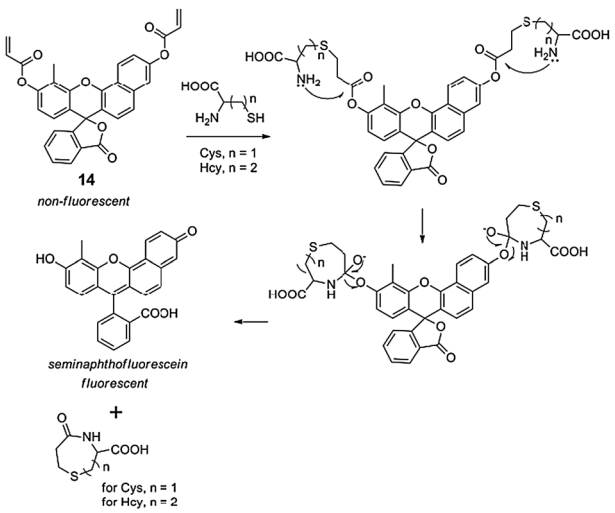

Fig. 14 Sensing of Cys by a tandem conjugate addition-intramolecular cyclization reactions.

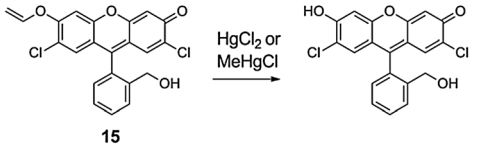

Fig. 15 Sensing of Hg^{2+}/methylmercury by mercury-promoted hydrolysis of vinyl ether.

A fluorescent chemodosimeter for cysteine detection was developed by Yang and co-workers based on a tandem conjugate addition–intramolecular cyclization reaction with seminaphthofluorescein (SNF) bis-acrylate **14** (Fig. 14),[22] the method exhibited an excellent selectivity for cysteine over other biothiols such as homocysteine and glutathione. The fluorescence intensity at 621 nm increases nearly proportional to the Cys concentration up to 10 μM, and, as low as 0.2 μM Cys can be readily detected. The excellent selectivity for cysteine over other biothiols comes from the preference of forming a 7-membered ring product in the intramolecular cyclization step.

On the basis of the classical oxymercuration reaction for carbon–carbon double bond, Ahn and co-workers reported a turn-on fluorescent probe **15** for mercury species (Fig. 15).[23] Fluorescein-derived vinyl ether **15** undergoes the mercury-promoted hydration to generate the corresponding hemiacetal, which is subsequently hydrolyzed to release the highly fluorescent product of the fluorescein derivative. According to the mechanism, the organomercury intermediate (RHgCl) may further promote the hydrolysis process, which showed the 1 : 1 reaction stoichiometry, whereas inorganic mercury species can hydrolyze two molar equivalents of the probe. A linear fluorescence response to the concentration of Hg^{2+} ranging from 1.0×10^{-9}–1.0×10^{-5} M or 0.2–2000 ppb was observed, and the detection limit was evaluated to be below 1 ppb level. Also, probe **15** exhibited sensitivity toward methylmercury. The probe was successfully used for the fluorescence imaging of methylmercury present in mammalian cells and vertebrate organisms.

Utilizing the Pd(0)-catalyzed Tsuji–Trost reaction, in which an allyl ether reacts with Pd(0) to generate an electrophilic (*p*-allyl)-Pd intermediate and an alkoxy fragment (Fig. 16), sensor **16**,[24] which is non-fluorescent, thus undergoes deallylation through Pd(0) catalysis under the conditions of pH 10 borate buffer solutions, giving rise to the highly fluorescent fluorescein species. And since Pd^{2+} can be readily reduced to Pd(0) by using *tris*-(2-furyl) phosphine and $NaBH_4$ as reducing agents, this probe therefore could also detect small quantities of Pd^{2+} species.

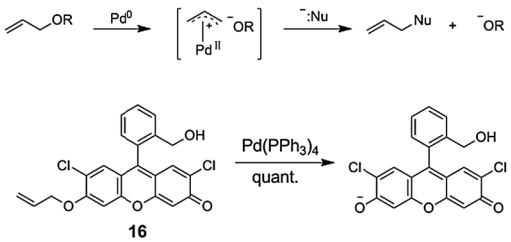

Fig. 16 Mechanism of Pd(0)-mediated cleavage of allyl ether and sensing of Pd(0) by probe **16**.

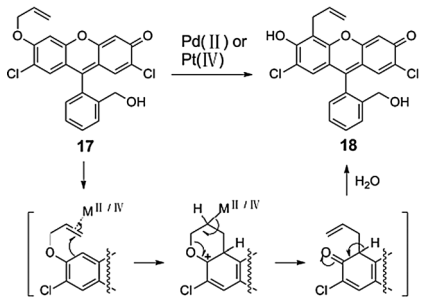

Fig. 17 Sensing of Pd^{2+} and Pt^{4+} by catalytic Claisen rearrangement in **17**.

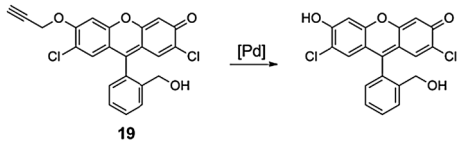

Fig. 18 Sensing of Pd species by catalytic depropargylation in **19**.

Claisen rearrangement was also adopted in the same probe for determination of $Pd^{2+/4+}$ and Pt^{4+} by Koide and co-workers (Fig. 17).[25] Among 21 common metal species including Pd(0), both $Pd^{2+/4+}$ and Pt^{4+} exclusively promoted this rearrangement at 50 °C after 4 h in 1 : 4 DMSO/pH 10 buffer, resulting in the transformation from nonfluorescent **17** to strong fluorescent **18**. Under optimized detection conditions, a linear fluorescence response depending on the concentration of Pd^{2+} in the range of 50 ppb to 5 ppm was observed. This method could be applied in the pharmaceutical industry, the environment, and Pd/Pt quality control.

The alkyne group could also be engineered into the same fluorophore architecture to design the fluorescein-based propargyl ether derivative **19** (Fig. 18),[26] which displays fluorescence enhancement for palladium species in the typical oxidation states of 0, +2 and +4 without additional reagents. When **19** was treated with $PdCl_2$ in water containing 10% CH_3CN at room temperature, the nonfluorescent solution emitted green fluorescence. The detection limit is determined to be 0.03 μM. The chemosensor is specific to Pd^{2+} among 22 other metal species examined and is applied to monitor accumulated palladium in living organisms.

Taki and co-workers incorporated the tetradentate ligand tris[(2-pyridyl)-methyl]amine (TPA) into a reduced form of a fluorescein platform through a benzyl ether linkage as an off–on fluorescent probe for Cu^+ (Fig. 19).[27] All of the spectroscopic measurements on **20a** or **20b** were performed under aerobic conditions in an aqueous buffer solution (50 mM HEPES, pH 7.20) containing 2 mM glutathione. Highly selective fluorescence changes

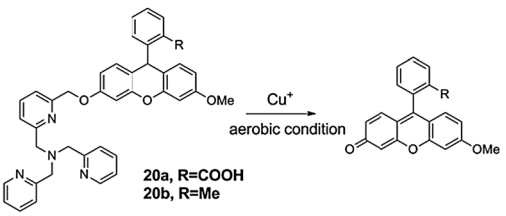

Fig. 19 Sensing of Cu^+ through metal-coordinated cleavage of benzyl ethers in **20**.

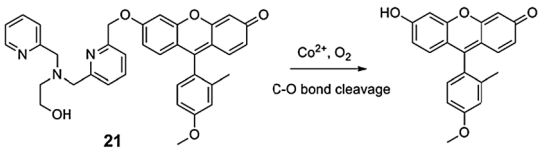

Fig. 20 Reaction-based Co^{2+}-selective fluorescent indicator **21**.

were observed upon addition of Cu^+ over Mn^{2+}, Co^{2+}, Ni^{2+}, Fe^{2+}, and Zn^{2+}, along with the cleaved C–O bond of the benzyl ether of **20a** and **20b**. The Cu^+ recognition process of the probes was not significantly influenced by other coexisting metal ions and **20b** was successfully applied to visualize Cu^+ in living cells.

Chang and co-workers incorporated a polypyridine-based "N_3O" type ligand into the phenol group of a fluorescein platform through a benzyl ether linkage as an off–on fluorescent probe for Co^{2+} in the medium of 50 mM Tris buffer at pH 7.4 in the presence of 5 mM glutathione (GSH) to mimic intracellular conditions (Fig. 20).[28] In the absence of Co^{2+}, blocking the xanthenone-ring phenol with the "N_3O" receptor results in a weakly fluorescent dye, however, under aerobic conditions, a reaction exploiting cobalt-mediated oxidative C–O bond cleavage affords a selective turn-on fluorescent behavior for paramagnetic Co^{2+} in water and in living cells. The fluorescence response of **21** is highly Co^{2+} selective over the cellular concentrations of Mg^{2+} and Ca^{2+}, or other transition metal ions including Mn^{2+}, Ni^{2+}, Fe^{3+}, Fe^{2+}, Cu^{2+}, Cu^+ and Zn^{2+}.

H_2S can undergo nucleophilic reaction twice, whereas other thiols such as cysteine are monosubstituted thiols that can only undergo nucleophilic reaction once. On the basis of this property, Xian's group reported a H_2S-mediated benzodithiolone (**23**) formation with probe **22** under mild conditions (Fig. 21).[29] This reaction proved to be selective for H_2S and it did not proceed with other biological thiols including cysteine and glutathione. As a free probe, **22** is colorless and nonfluorescent in aqueous phosphate-buffered saline solution (pH 7.4). Upon addition of NaHS, a spontaneous cyclization occurred to release a fluorescein-based fluorophore resulting in dramatic increases in the fluorescence intensity, and the fluorescence signal was linearly related to the concentration of NaHS. Also, probe **22** can be used for the selective detection of H_2S in plasma and cells such as cultured COS7 cells.

Thereafter, Xian and co-workers further developed a Michael acceptor-based fluorescent probe for hydrogen sulfide (H_2S).[30] The design was based on a Michael addition of H_2S followed by an intramolecular cyclization to release the fluorophore (Fig. 22). The experiments demonstrated that in pH 7.4 phosphate buffer

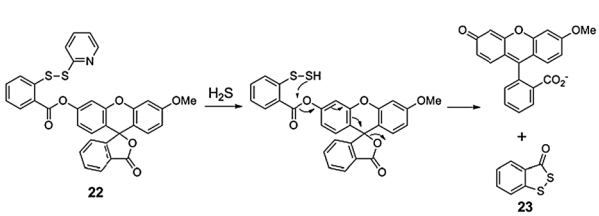

Fig. 21 Sensing of H_2S by twice nucleophilic reaction in probe **22**.

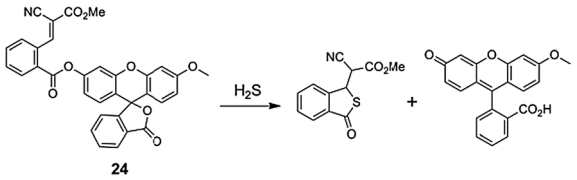

Fig. 22 Sensing of H_2S by tandem reaction of Michael addition and intramolecular cyclization.

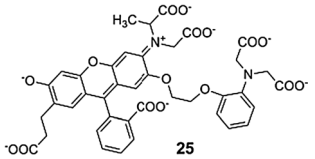

Fig. 23 Rhodafluor-based probe for Ca^{2+}.

solution, the turn-on response of probe **24** was selective for H_2S over the majority of biologically relevant thiols such as cysteine and glutathione and the probe could be used for the detection of H_2S in the presence of a high concentration of these two biological thiols. The detection limit for H_2S using probe **24** was found to be 1.0 μM. Probe **24** can be used for the detection of H_2S in cultured COS7 cells.

"Rhodafluor", also named as rhodol fluorophores, is a kind of hybrid involving elements of the closely related rhodamine and fluorescein in structure. Clarke and co-workers incorporated a tetracarboxylate chelating element similar to that of BAPTA (1,2-bis[2-aminophenoxy]ethane-*N*,*N*,*N*′,*N*′-tetraacetic acid), which is a well-established chelator for the Ca^{2+} ion, into the rhodafluor platform (Fig. 23).[31] The excitation and emission fluorescence spectra of the free probe, **25**, shifted from rhodamine-like fluorescence at 537 nm and 566 nm, respectively, to fluorescein-like fluorescence at 480 nm and 537 nm, respectively, in the presence of Ca^{2+}. The probe can be used in either the dual excitation or dual emission mode, and the value of these two ratios can be found by dual excitation and dual emission measurements. The probe was also insensitive to pH from 6.5 to 7.5 in the ratio mode assay.

Lippard and co-workers designed a chemosensor **26**, bearing a carboxylate moiety, which is negatively charged in neutral aqueous solution, on the di(2-picolyl)amine (DPA) unit for sensing of Zn^{2+} (Fig. 24).[32] The carboxylate group was expected to act not only as an enhancement to increase the bound affinity of the probe to zinc, but also to stabilize a partial positive charge on the nitrogen donor of the frame so that the binding of the zinc ion would in turn repel the positive charge leading to an increase in the population of the fluorescein-like aminoquinone mesomer

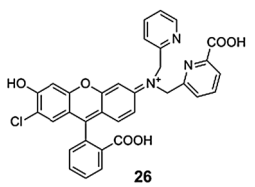

Fig. 24 Rhodafluor-based probe for Zn^{2+}.

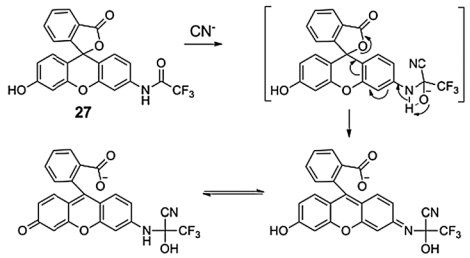

Fig. 25 Rhodafluor-based probe sensing of CN^- by formation of the carbonyl adduct.

form. Free **26** showed visible absorption and emission maxima at 514 and 540 nm, respectively, and displayed a hypsochromic shift of the absorption band at 495 nm with an emission at 523 nm in the presence of zinc ions. As a result, **26** behaved as a ratiometric zinc sensor and its fluorescence response can be measured by the ratio of emission intensities at 523 and 540 nm. Furthermore, the emission profile and zinc response of **26** were stable over pH values ranging from 5.5 to 9.0.

Guo and co-workers designed a rhodafluor-based chromo- and fluorogenic probe bearing a mono-trifluoroacetylamino binding unit for CN^- in MeOH–H_2O solution (8/2, v/v) over F^-, Cl^-, Br^-, I^-, AcO^-, SCN^-, N_3^-, ClO_4^-, NO_3^-, SO_4^{2-} and $H_2PO_4^-$ (Fig. 25).[33] The probe itself is colorless and nonfluorescent because of its spirocyclic structure, whereas ring-opening induced by CN^- gives rise to strong fluorescence emission at 520 nm and also clear color changes. The detection limit was measured to be 2.66×10^{-8} M, which is much lower than the World Health Organization (WHO)'s limit (1.9 μM) for drinking water.

Chemosensors derived from the xanthene ring at positions 4 and/or 5

A water-soluble "turn-on" fluorescein-based sensor was reported by Lippard and co-workers which exhibits high selectivity and sensitivity for Hg^{2+} (Fig. 26).[34] In aqueous solution (pH 7.0, 50 mM piperazine-*N*,*N*′-bis(2-ethanesulfonic acid) (PIPES), 100 mM KCl buffer), the fluorescence of sensor **28** is weak due to the photoinduced electron transfer (PET) effect from the lone pair of the aniline nitrogen atom to the excited state of the fluorescein. Upon addition of Hg^{2+}, the emission and absorption spectra of sensor **28** exhibited a slight shift, along with ~5-fold enhancement of the emission; this was attributed to disruption of the PET process. The Hg^{2+} response of **28** is unaffected in a background of environmentally relevant alkali and alkaline earth

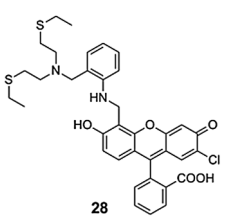

Fig. 26 Turn-on fluorescein-based probe for Hg^{2+}.

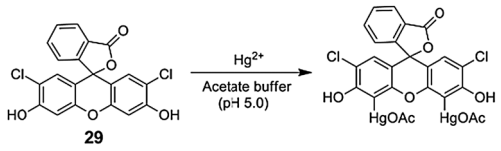

29

Fig. 27 Fluorescein-based chemodosimeter for Hg^{2+} by mercuration.

metals including Li^+, Na^+, Rb^+, Mg^{2+}, Ca^{2+}, Sr^{2+} and Ba^{2+}. Transition metal ions examined such as Cr^{3+}, Mn^{2+}, Fe^{2+}, Co^{2+}, Ni^{2+}, Cu^{2+}, Zn^{2+}, Cd^{2+} and Pb^{2+} also show almost no significant changes in the fluorescence intensity with the exception of Cu^{2+}.

Chang and co-workers developed a simple chemodosimetric signaling system, based on a readily available dichlorofluorescein, for the selective determination of Hg^{2+} ions in aqueous solutions (Fig. 27).[35] Dichlorofluorescein **29** exhibited characteristic absorption bands at 475 nm of shoulder peak and 505 nm of maximum absorption wavelength in acetate-buffered aqueous solution (pH 5.0) containing 10% DMSO. Upon treatment with Hg^{2+} ions, the absorption bands at 475 and 505 nm were gradually decreased and red-shifted to 483 and 533 nm, respectively, and the strong emission band around 528 nm was effectively quenched upon treatment with Hg^{2+} ions. Signaling was due to the selective mercuration at the 4, 5-positions of the xanthene ring. **29** could be used to measure the concentration of Hg^{2+} ions in the micromolar range (detection limit 7.5×10^{-6} M) over other common interfering metal ions in an aqueous environment.

Series of fluorescent sensors for Zn^{2+}, **30a–d,** have been synthesized and characterized by Lippard and co-workers (Fig. 28).[36] A 3- to 5-fold fluorescence enhancement is observed under simulated physiological conditions (50 mM PIPES, 100 mM KCl, pH 7) corresponding to the binding of the Zn^{2+} to the sensors of **30a** and **30b**, respectively, which inhibit a photoinduced electron transfer (PET) quenching pathway. **30a** and **30b** are selectively for Zn^{2+}, 5 mM of biologically relevant Ca^{2+} and Mg^{2+} produce no change in their fluorescence, and other first-row transition metal ions including Cu^+, Cu^{2+}, Ni^{2+}, Co^{2+}, Fe^{2+}, and Mn^{2+} quench the fluorescence.

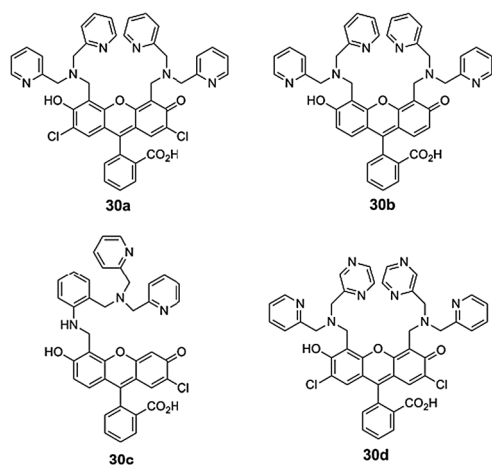
30a 30b 30c 30d

Fig. 28 Series of turn-on fluorescein-based probes for Zn^{2+}.

To further avoid possible proton interference due to retaining an appreciable affinity for Zn^{2+}, a second-generation of Zn^{2+}-selective sensor, **30c**, has been designed, synthesized and characterized by Lippard's group.[37] The probe integrated an aniline nitrogen into a chelating ligand containing a di(2-picolyl)amine (DPA) moiety. **30c** has excitation and emission wavelengths in the visible range ($\sim$500 nm), a dissociation constant (K_d) for Zn^{2+} of less than 1 nM and high quantum yields (Φ = $\sim$0.4), making it well suited for biological applications. A 5-fold fluorescence enhancement is observed under simulated physiological conditions when binding of the Zn^{2+} to the sensor, which also inhibits a photoinduced electron transfer (PET) quenching pathway. The key feature of **30c** is that the aniline nitrogen of the unmetalated fluorophore has a lower pK_a than the aliphatic nitrogen of **30a** and **30b**, making it less sensitive to protonation under physiological conditions. Because the background fluorescence from the free probe is diminished, **30c** is more sensitive than **30a** and **30b**.

Later, Lippard and co-workers further modified **30a** by substitution of one pyridine by pyrazine at each DPA unit to afford the new probe, **30d**,[38] which exhibits low background fluorescence and hence a higher zinc-responsive fluorescence "turn-on" behavior due to the lower pK_a value of the quenching units compared to that of **30a**. Most interestingly, **30d** exhibits a distinct two-step fluorescence turn-on upon binding 1 *vs.* 2 equiv. of zinc, which can be applied to quantify zinc concentration levels and the amount of zinc released from granules upon stimulation. Moreover, **30d** can selectively stain mobile zinc in the secretory granules of Min6 cells.

Lippard and co-worker also presented another set of Zn^{2+}-selective probes **31a** and **31b** containing one or two 8-aminoquinoline units on the xanthene moiety (Fig. 29).[39] These probes displayed micromolar K_d values for Zn^{2+} at pH 7 (50 mM PIPES, 100 mM KCl) and were ready to detect Zn^{2+} in the presence of biologically relevant concentrations of Na^+, K^+, Mg^{2+}, and Ca^{2+}, displaying excellent selectivity for Zn^{2+}. Due to their low background fluorescence and highly emissive Zn^{2+} complexes, **31a** and **31b** have a large dynamic range, with $\sim$42- and $\sim$150-fold fluorescence enhancements upon Zn^{2+} coordination, respectively.

Wang and Li *et al.* reported a novel switch-on fluorescent system which was based on restricting the rotation of C=N bonds by complexation of cations (Fig. 30). The fluorescence of compound **32** is largely enhanced by adding Cd^{2+}, differentiated from other cations such as NH_4^+, Li^+, Na^+, K^+, Mg^{2+}, Ca^{2+}, Mn^{2+}, Pb^{2+}, Fe^{2+}, Co^{2+}, Ni^{2+}, Cu^{2+}, Hg^{2+}, and Zn^{2+}, indicative of its

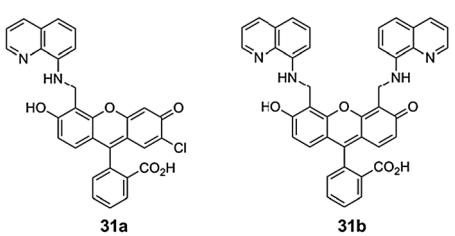
31a 31b

Fig. 29 Turn-on fluorescein-based probes for Zn^{2+} by appending aminoquinoline units as receptors.

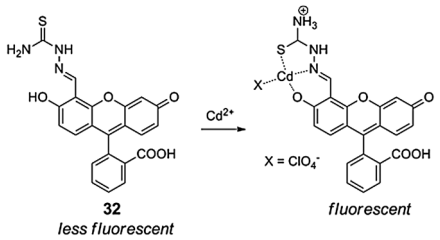

Fig. 30 Chemosensor for Cd^{2+} by restricting the rotation of C=N bond.

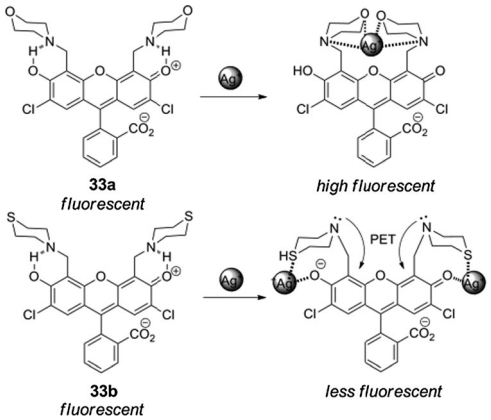

Fig. 31 Fluorescein-based probes for Ag^+ by appending morpholine or thiomorpholine units.

selectivity to Cd^{2+} under physiological conditions (50 mM HEPES, 100 mM KCl, pH 7.0).[40] This significantly enhanced fluorescence is probably due to the formation of a 1 : 1 complex in which the rotation of acyclic C=N is frozen. The sensitivity of compound **32** to Cd^{2+} was demonstrated in living cells, indicating its potential application for Cd^{2+} diagnoses in clinics.

Yoon and co-workers designed probes of fluorescein derivatives, **33a** and **33b**, bearing a fluorescent chromophore to which are appended morpholine and thiomorpholine substituents, respectively (Fig. 31).[41] **33a** and **33b** display extremely selective binding of Ag^+ among the metal ions examined at pH 7.4. Chemosensor **33a** shows a selective fluorescence enhancement with Ag^+. On the other hand, the fluorescence of chemosensor **33b** is quenched and a light yellow to pink color change takes place upon addition of Ag^+. The opposite fluorescence changes in **33a** and **33b** promoted by the addition of Ag^+ are attributed to completely different metal cation binding modes of these substances. For probe **33b**, two Ag^+ ions chelate with sulfurs of the two thiomorpholine rings and the phenolic oxygens of fluorescein. The consequence of this complexation mode is that intramolecular hydrogen bonding between the phenolic hydrogens and the benzylic amines is eliminated. This releases tertiary amine groups that can now participate in photo-induced electron transfer (PET) quenching of emission from the fluorescein chromohore. On the other hand, the fluorescence enhancement of **33a** is likely to be caused by one Ag^+ coordination with nitrogens of the two morpholine donors, thus the strong interactions between the benzylic amines and Ag^+ block the PET quenching and result in a fluorescence enhancement.

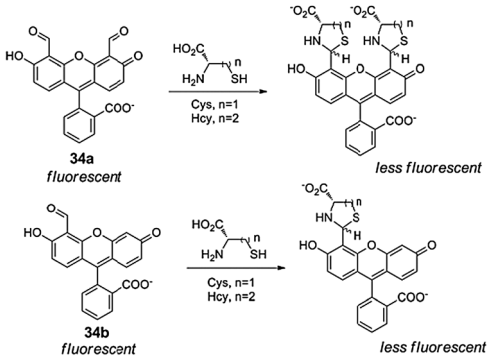

Fig. 32 Sensing of Cys and Hcy by formation of thiazoline and thiazinane derivatives.

On the basis of the well-known cyclization reactions of β-/γ-aminoalkylthiols (containing both SH and NH_2 groups) with organic aldehydes, which form the thiazolidine and thiazinane derivatives, colorimetric and high selectivity fluorescent probes for thiol-containing amino acids were developed by Strongin and co-workers (Fig. 32).[42] Upon addition of Cys or Hcy to a solution of **34a** or **34b**, a solution color change from bright yellow to brownish-orange can be observed, resulting in fluorescence quenching.

Yoon and co-workers reported a new fluorescein-based fluorescent probe **35**, for the detection of thiol-containing molecules with high selectivity and sensitivity (Fig. 33).[43] In 4-(2-hydroxyethyl)-1-piperazineethanesulfonic acid (HEPES) buffer (20 mM, pH 7.4, 1% CH_3CN), addition of thiols such as Cys, Hcy, and GSH led to a 1,4-addition reaction of α,β-unsaturated ketone in **35** followed by the spiro-ring-opening of fluorescein fluorophore. By fluorescence titration experiments, the detection limits were estimated to be less than 50 nM for Cys, about 100 nM for Hcy, respectively. **35** alone showed little change in fluorescence intensity over the pH 2.7–10.0, and responded to thiols under neutral and basic conditions. Moreover, *in vivo* studies proved that **35** could enter cells and zebrafish, and react with thiols to form the fluorescent product.

Yoon and co-workers also introduced **34b** as a cyanide selective chemodosimeter over various anions, such as CN^-, AcO^-, F^-, Cl^-, Br^-, I^-, $H_2PO_4^-$, HSO_4^-, NO_3^- and ClO_4^- in acetonitrile–HEPES buffer (9 : 1, v/v, 0.01 M pH 7.4) (Fig. 34).[44] The mechanistic study revealed that the aldehyde group in salicylaldehyde was activated toward nucleophilic attack of CN^- followed by intramolecular hydrogen transfer with the phenol proton, as a consequence, **34b** displayed both a colorimetric change and a ''Off–On'' type green fluorescence with cyanide.

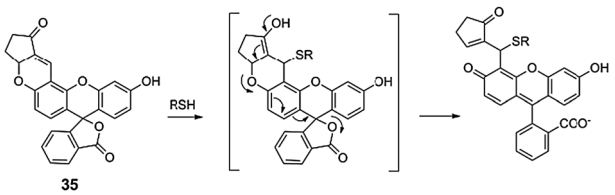

Fig. 33 Mechanism of response of **35** to thiols in aqueous solution.

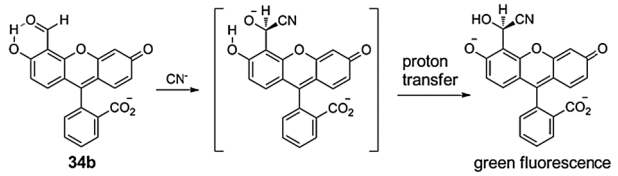

Fig. 34 Turn on sensing of CN^- with fluorescein-aldehyde **34b**.

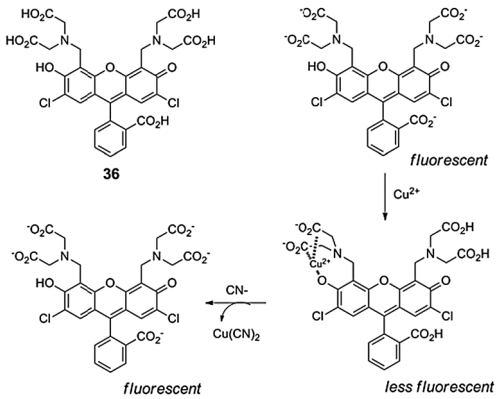

Fig. 35 Turn-on fluorescein-based ensemble probe for CN^-.

The practical use of the probe was also demonstrated by its application to the detection of cyanide in the living cells.

Inspired by the fact that cyanide is known to react with copper ions to form very stable $Cu(CN)_2$ species, Yoon and co-worker devised the **36**-Cu^{2+} complex as a ''Off–On'' type fluorescent ensemble sensor of cyanide (Fig. 35),[45] in which the fluorescent ligand **36** displayed a fluorescence quenching effect with Cu^{2+} and the addition of cyanide to this solution induced ''Off–On'' type fluorescence enhancement. The complex **36**-Cu^{2+} can monitor cyanide at pH 7.4 in 100% aqueous system, and anion selectivity experiments indicated that the emission from **36**-Cu^{2+} was unaffected by SCN^-, AcO^-, F^-, Cl^-, Br^-, I^-, $H_2PO_4^-$, HSO_4^-, NO_3^- and ClO_4^-. The probe was also used for fluorescent imaging of cyanide *in vivo C. elegans*.

Guo *et al.* have presented a 4-(*N*,*N*-dimethlyamino) benzamide-fluorescein probe, **37**,[46] as a ratiometric fluorescent probe for CN^- based on the FRET mechanism (Fig. 36), which exhibits a clear CN^--induced change in the intensity ratio of the two well-separated emission bands of the 4-(*N*,*N*-dimethylamino)benzamide group as a donar and fluorescein fluorophore as an acceptor. In aqueous solution (0.1 M HEPES, pH 7.2), upon addition of CN^-, the donor

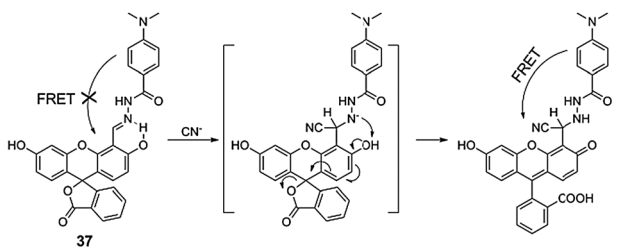

Fig. 36 FRET-based ratiometric chemodosimeter for CN^-.

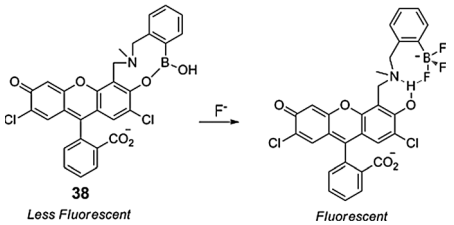

Fig. 37 Fluorescein-based probe for F^-.

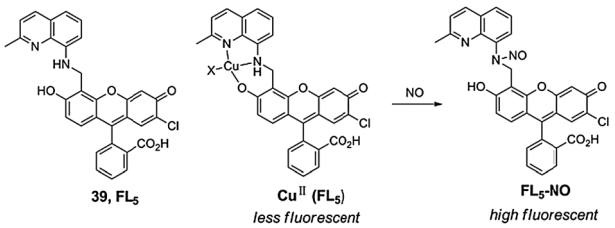

Fig. 38 Turn-on fluorescein-based ensemble probe for NO by nitrosation reaction.

emission at 450 nm decreased, and the acceptor emission gradually increased in intensity with a substantial red shift from 530 nm to 550 nm, which was resulted from the ring-opened form of the fluorescein unit in **37** induced by the nucleophilic attack of CN^-. The sensor is selective for CN^- over other anions, except for F^-, AcO^- and $H_2PO_4^-$, which interfere mildly due to the deprotonation reaction of **37** by these weakly basic anions to partly trigger the ring-opening of the fluorescein unit.

Yoon and co-workers developed a new fluorescein derivative **38** bearing a boronic acid group as a fluorescent chemosensor for F^- (Fig. 37).[47] **38** displayed a selective fluorescence enhancement with a fluoride ion among the halide ions. This high F^- selectivity is due to the fluorescein core structure and the boron–fluoride interaction. The relatively weak interaction between benzylic nitrogen and boron may be attributed to the moderate fluorescence emission of **38** by the PET process from the benzylic nitrogen to fluorescein fluorophore. Upon the addition of a fluoride ion, the phenolic hydrogen can make a strong hydrogen bond with fluoride as well as benzylic amine, which blocks the PET mechanism, resulting in fluorescence enhancement.

A fluorescein-based ligand, **39** (**FL_5**), which was used as a framework for Cu^{2+}-based complexes was synthesized by Lippard and co-workers (Fig. 38).[48] The ensemble probe could serve as biosensor for nitric oxide at a physiologically relevant pH. The low fluorescence of a Cu^{2+} complex, Cu-**FL_5**, generated *in situ* by reaction of **39** with $CuCl_2$, exhibits a significant increase in fluorescence upon addition of NO in pH 7.0 buffered aqueous solution. Turn-on emission of Cu-**FL_5** by NO occurs by reduction of Cu^{2+} to Cu^+, forming NO^+, which nitrosates **39** to create an additive of **FL_5-NO**, triggering fluorescence enhancement, as revealed by spectroscopic and product analyses of the reaction. The fluorescence response to NO of the Cu-**FL_5** complex is specific over other biologically relevant reactive species such as $O_2^{\bullet -}$, H_2O_2, NO_2^-, NO_3^-, HNO, $ONOO^-$, and ClO^-.

Nam and co-workers reported a novel method for the detection of fluorescence in response to the presence of intracellular H_2O_2

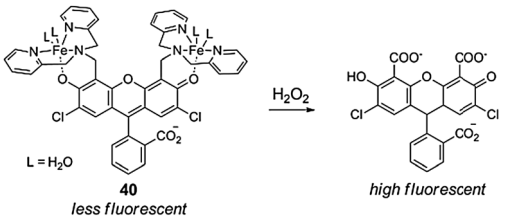

Fig. 39 Ensemble chemodosimeter for H_2O_2 by H_2O_2-triggered intramolecular oxidative cleavage.

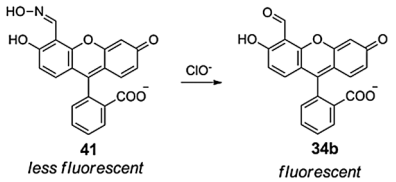

Fig. 40 Chemodosimeter for ClO^- by removing the C=N bond isomerization.

(Fig. 39).[49] The complex probe platform, **40**, was readily constructed by complexation of an iron ion and **30a**. Paramagnetic iron in the complex quenched the fluorescence emission of the fluorophore, whereas activation by H_2O_2 triggered intramolecular oxidative cleavage between the iron ionophore and the fluorophore to produce a fluorescence turn-on signal. The detection limit for H_2O_2 was determined to be 29 μM and the unique mechanism affords exceptional selectivity for H_2O_2 over other ROSs. Moreover, this H_2O_2 probe is applicable to live cell imaging and has the ability to detect intracellular H_2O_2 at the lysosome.

Li and co-workers proposed a new design strategy for the development of fluorescent turn-on chemodosimeters for ClO^- by the mechanism of removal, but not the general restricting, of the C=N isomerization (Fig. 40). **41** displayed high sensitivity and extremely high selectivity for ClO^- in 10 mM HEPES buffer (pH 7.05) containing 10% (v/v) DMSO solution based on the deprotection reaction in an oxime group to release an aldehyde, making it a candidate of great potential for the selective detection of ClO^- in the presence of other common ions and oxidants. The fluorescence images indicated that **41** can penetrate the cell membrane and be used for the imaging of ClO^- in living cells and *in vivo* potentially.[50]

Chemosensors derived from the xanthene ring at positions 3 and/or 6

Generally, in fluorescein and rhodamine fluorophores, the hydroxyl and amino groups or their derivatives are attached at positions 3 and 6. Therefore, molecular design can be conducted by incorporating any latent groups at position 3 and/or 6, where these groups can be transformed to a hydroxyl or an amino group by a specific analyte to release fluorescein and rhodamine fluorophores.

Based on the chemical conversion of arylboronates to the phenols by the reactive oxygen species, Chang and co-workers devised a new water-soluble turn-on optical probe (Fig. 41), **42**,[51] for hydrogen peroxide (H_2O_2) under simulated physiological

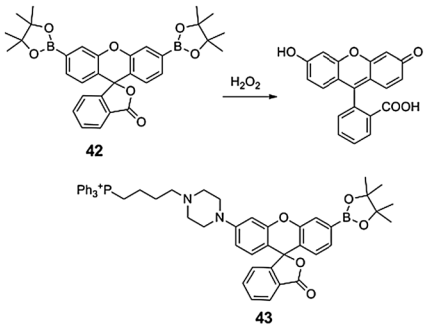

Fig. 41 Boronate-based turn on probes **42** and **43** for H_2O_2.

conditions (20 mM HEPES buffer, pH 7.0), that exhibited high selectivity and a dynamic range for this small molecule over competing biological ROS like superoxide ($O_2^{\bullet -}$), nitric oxide (NO), hydroxyl radical ($^{\bullet}OH$), and lipid alkylperoxides. Furthermore, **42** was membrane-permeable and could respond to micromolar changes in intracellular H_2O_2 concentrations within living mammalian cells.

Further, based on the same mechanism, by employing the "rhodafluor" platform, Chang and co-workers further engineered a latent fluorophore, **43**, by incorporating a boronate group and a lipophilic phosphonium group, which can serve as a mitochondrial-targeting moiety, onto xanthene. **43** is featured by its bifunctional abilities of both targeting the mitochondria and responding to H_2O_2 in living cells.[52]

On the basis of the FRET mechanism, Chang and co-workers developed a ratiometric fluorescent H_2O_2 sensor **44**, which conjugates a coumarin moiety as a donor and a boronate-protected fluorescein as a latent acceptor (Fig. 42).[53] Under simulated physiological conditions, sensor **44** itself showed blue donor emission upon excitation of the coumarin chromophore. However, upon addition with H_2O_2 to generate the open, colored, and fluorescent fluorescein moiety, the acceptor showed a strong absorption in the coumarin emission region. Changes in the concentration of H_2O_2 can be detected by measuring the ratio of blue and green fluorescence intensities. This FRET-based probe shows high selectivity for H_2O_2 over other ROS. Further experiments with viable mitochondria show that **44** can be employed in detection and quantification of endogenous H_2O_2 production.

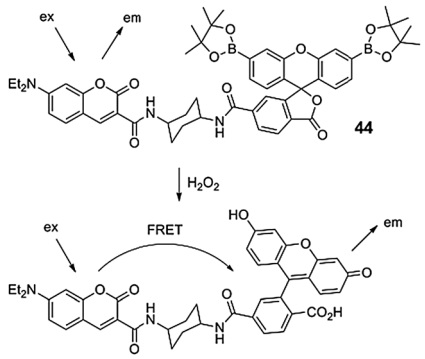

Fig. 42 FRET-based ratiometric chemodosimeter for H_2O_2.

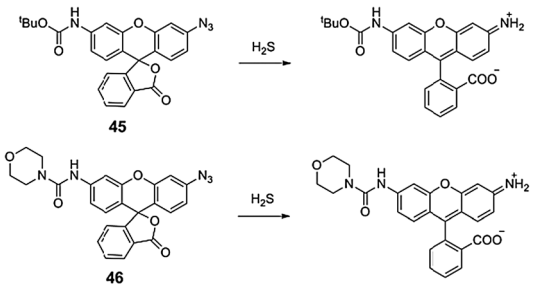

Fig. 43 Probes for H_2S by H_2S-mediated reduction of azides.

Exploiting the H_2S-mediated reduction of azides to amines, Chang and co-workers reported a pair of new rhodamine-based fluorescent probes for selective imaging of H_2S in living cells (Fig. 43).[54] In aqueous solutions buffered at physiological pH (20 mM HEPES, pH 7.4), **45** and **46** respond to H_2S by a "turn-on" fluorescence signal enhancement and display high selectivity for H_2S over other biologically relevant reactive sulfur, oxygen, and nitrogen species. In addition, **45** and **46** can be used to detect H_2S in both water and live cells, providing a potentially powerful approach for probing H_2S chemistry in biological systems. The *in vitro* detection limit for H_2S using **45** and **46** was found to be 5–10 μM.

Chemosensors from derivative reactions at position 2′

Nagano and co-workers designed and synthesized fluorescent probes, **47a** and **47b**, for the selective detection of highly reactive oxygen species (hROS) generated in mitochondria in real time (Fig. 44).[55] Probe **47a** itself gave almost no fluorescence, owing to PET-mediated quenching. Reaction with hROS could cause cleavage of the ether moiety, affording a strong fluorescent product in an aqueous environment. **47a** has excellent properties for biological applications, including tolerance to autoxidation and photobleaching during laser irradiation for fluorescence microscopy.

Nagano and co-workers prepared the tetramethylrhodamine based fluorescent probe **48**, a rhodamine spiro-thioether scaffold, for detecting hypochlorous acid with good selectivity (Fig. 45).[56] Hypochlorous acid oxidized the thioether group in **48** to generate the corresponding sulfonate, this process led to the opening of the spiro-ring system in **48**, resulting in a concomitant increase in fluorescence. Probe **48** also exhibited high tolerance to autoxidation and excellent selectivity for HOCl over other ROS/RNS. Importantly, **48** can work in 99.9% aqueous solution at pH 7.4 and was

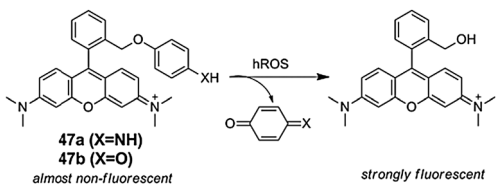

Fig. 44 Sensing of hROS by a reaction of oxidative cleavage of the ether.

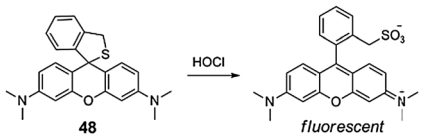

Fig. 45 Sensing of HClO through an oxidative opening the spiro-thioether ring.

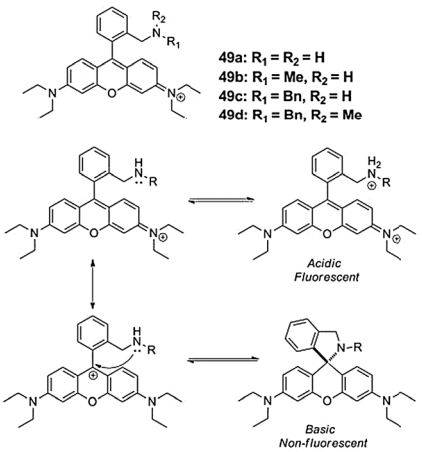

Fig. 46 Rhodamine spiro-deoxylactam-based probes for H^+.

confirmed to be able to detect hypochlorous acid being generated inside phagosomes in real time.

Dyer and co-workers synthesized a series of structurally similar rhodamine B based chemosensors, the so-called "rhodamine spiro-deoxylactam" (Fig. 46),[57] which can behave differently for the detection of the pH in solution, depending upon the nucleophilicity and steric hindrance of the amine moiety attached. In acid solutions, **49a–c** are present in spiro-ring opening state with strong fluorescence. However, under basic conditions, they predominate as spiro-cyclic scaffolds, which quench the fluorescence of the rhodamine B fluorophore. Probe **49d**, however, the tertiary amine moiety is incapable of undergoing intramolecular cyclization, and therefore, its fluorescence is controlled by PET from the amine moiety.

Han and co-workers developed a chromogenic and fluorogenic assay of a nerve agent simulant based on reactive organophosphate triggered irreversible opening of the spiro-ring of the deoxylactam of **50** (Fig. 47).[58] Upon addition of diethyl chlorophosphate, the solution, **50** quickly turned into red color attributed to the formation of a highly fluorescent product resulted from opening of the deoxylactam ring. In DMF solvent containing TEA (3%, v/v), as low as 25 ppm of diethyl chlorophosphate can be detected. Further, the assay system allows us

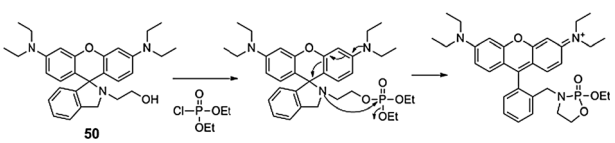

Fig. 47 Sensing of organo-phosphate by ring opening of rhodamine spiro-deoxylactam-based probe **50**.

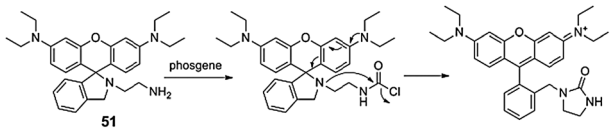

Fig. 48 Sensing of phosgene by ring opening of rhodamine spiro-deoxylactam-based probe **51**.

to detect reactive organophosphates with the aid of instruments or possibly with the "naked eye".

Later, by the same scaffold, they developed **51** to sense triphosgene (Fig. 48).[59] Under the assay conditions (DMF solvent containing 3% TEA in volume), **51** could detect triphosgene with superior sensitivity with a detection limit of 50 nM. The assay proceeds *via* analyte triggered opening of the deoxylactam ring of **51** and affords deep-colored and highly fluorescent species. Given the promptness of the color formation, low background interference, and high sensitivity of this assay, **51** is also attractive for on-spot detection of gaseous phosgene with routine instruments or the "naked eye".

Lin and co-workers created a fluorescent turn-on probe for Cu^{2+} based on the copper-mediated dihydrorosamine oxidation reaction (Fig. 49), and the probe has been employed to sense Cu^{2+} in 20 mM HEPES buffer at pH 7.4 (containing 40% CH_3CN as a cosolvent).[60] No marked changes in the emission were noted upon addition of the representative species such as Ag^+, Al^{3+}, Ca^{2+}, Cd^{2+}, Co^{2+}, Fe^{2+}, Fe^{3+}, Hg^{2+}, Mn^{2+}, Ni^{2+}, Pb^{2+}, Zn^{2+}, F^-, NO_2^-, H_2O_2 + horseradish peroxidase (HRP), and $^{\bullet}OH$, indicating that **52** has a high selectivity for Cu^{2+}. In addition, **52** showed high sensitivity toward Cu^{2+} with a detection limit of 2.61×10^{-7} M. And furthermore, it was proposed that the oxidation reaction likely proceeds by a copper redox mechanism.

Ma's group and Zheng's group have synthesized independently a rhodamine thiolactone (Fig. 50), **53**, as a Hg^{2+}-specific probe.[61,62] The design strategy of the probe was based on the consideration that the thiol atom, which linked with the spirocarbon atom, would provide a direct attacking center for the thiophilic Hg^{2+} and was anticipated to attain a high sensitivity for the sensing. Besides, **53** bears advantages of more stability

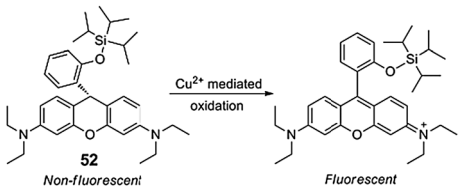

Fig. 49 Fluorescent turn-on probe for Cu^{2+} based on the copper-mediated dihydrorosamine oxidation.

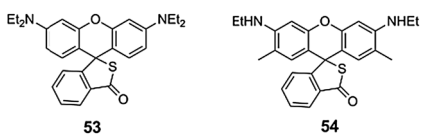

Fig. 50 Rhodamine thiolactone probes for Hg^{2+}.

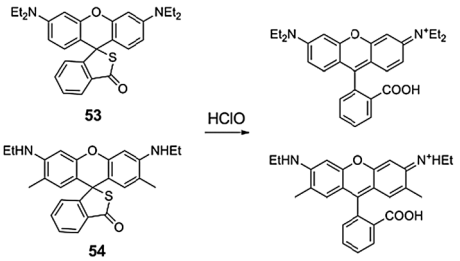

Fig. 51 Rhodamine thiolactone probes **53** and **54** for HClO.

in its spirocyclic form due to the stronger nucleophilic ability of the S atom and thus would show high tolerance to pH. It was revealed that **53** showed high sensitivity with a detection limit of 2 ppb and high selectivity over other metal ions. In addition, the probe retained its cyclic ring in a pH range of 1–11. At nearly the same time, **54** was also applied for *in vivo* imaging of Hg^{2+} using *C. elegans* by Yoon and co-workers.[63]

The functional sulfur element in the framework of **53** was also found to selectively react with hypochlorous acid over other reactive oxygen species, leading to the recovery of fluorescence which resulted from the opening of the thiospiro-cycle and release of free rhodamine B (Fig. 51).[64] Therefore, **53** was successfully applied to visualize hypochlorous acid generated in neutrophils of human blood. In addition, rhodamine 6G thiolactone, **54**, was also reported to detect hypochlorous acid induced in mucosa of live animals by the same chemical pathway.[65]

A Se atom was also incorporated into the spirocyclic rhodamine skeleton by Ma and co-workers to prepare a rhodamine B selenolactone, **55**, as a Hg^{2+} and Ag^+-specific fluorescent probe (Fig. 52).[66] The Hg^{2+}- or Ag^+-induced spirocyclic opening was suggested to be irreversible and proceed through in a way that the selenium atom of the probe binds selectively with Hg^{2+} or Ag^+ due to the high affinities of Se–Hg and Se–Ag, and the subsequent complexation of Hg^{2+} or Ag^+ promotes hydrolytic cleavage of the selenolactone bond, causing the release of rhodamine B and the retrieval of the fluorescence, for which the changes in intensity were found to be directly proportional to the concentration of 0.1–5 μM Hg^{2+} and 0.1–10 μM Ag^+ with detection limits of 23 nM Hg^{2+} and 52 nM Ag^+. Most notably, the probe is capable of sensing Ag^+ in the presence of a high concentration of Cl^- since Se has a stronger binding ability toward Ag^+ than Cl^-. The probe was also reported, by Yoon and co-workers, to be capable of monitoring methylmercury and was successfully applied to image Hg^{2+} and CH_3HgCl in zebra fishes.[67]

Inspired by the fact that the cellular functions of nitric oxide are concerned with the interaction between NO and the SeH groups of selenoproteins, which involving the formation of Se–NO bonds, Ma and co-workers further applied **55** to study its fluorescence response

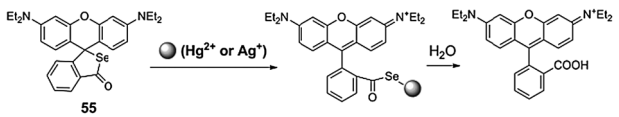

Fig. 52 Rhodamine B selenolactone for Hg^{2+} or Ag^+.

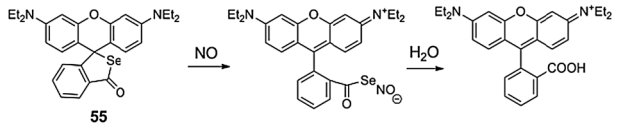

Fig. 53 Rhodamine B selenolactone probe **55** for NO.

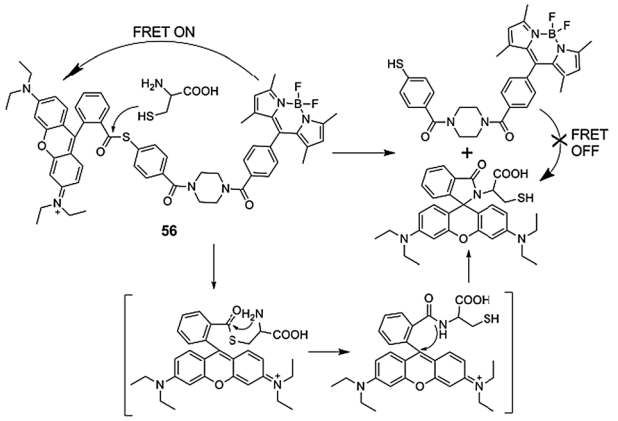

Fig. 54 Ratiometric fluorescent sensing of thiols by rhodamine thioester-based probe.

for NO (Fig. 53).[68] It was found that NO induced the opening of the selenolactone ring within a period of 15 minutes *via* a route in which an unstable intermediate containing the Se–NO bond was formed firstly, followed by the hydrolyzation into rhodamine B. A good linearity between the change in fluorescence intensities and the NO concentration in the range of 2.5 to 30 μM was observed with a detection limit of 38 nM. In addition, other common coexisting substances including other reactive oxygen/nitrogen species showed no obvious fluorescence response, indicating probe **55** might be a promising fluorescent probe for NO.

Lin and co-workers constructed a novel FRET-based ratiometric fluorescent thiol probe suitable for imaging in living cells.[69] The rhodamine thioester-base probe (Fig. 54), **56**, exhibited efficient energy transfer from BODIPY (donor) to rhodamine (acceptor), and only showed the emission of rhodamine at 590 nm with excitation at 470 nm. After adding Cys, the sulfhydryl group of Cys attacks the electrophilic carbon of the thioester group, and further the tandem reactions of *trans*-thioesterification and intramolecular rearrangement result in the cleavage of the FRET dyad and the switch-off of the FRET process. As a consequence, the intensity of the rhodamine emission at 590 nm gradually decreased with the concomitant growth of a new emission peak of BODIPY fluorophore at 510 nm. The detection limit of the probe was determined to be 8.2×10^{-8} M. In addition, the FRET-based ratiometric imaging of thiols in living cells by employing **56** has been demonstrated.

A new rhodamine spiro-scaffold with a six-membered reactive ring (Fig. 55) was developed by Zheng and co-authors by inserting a nitrogen atom in the known probe **57**,[70] which switched the recognition preference of the probe from Hg^{2+} to Cu^{2+}. This probe, **58**,[71] is shown to be an efficient "turn-on" fluorescent chemodosimeter for Cu^{2+} in a buffer solution of 3,3-dimethylglutaric acid/NaOH (10 mM in water/acetonitrile

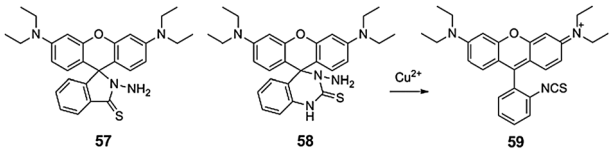

Fig. 55 Probe with ring expansion in traditional rhodamine spiro-lactam scaffold.

solution, 80 : 20, v/v) at pH 7.0, and, it also displays high selectivity toward Cu^{2+} in a neutral aqueous medium, and the fluorescence titration curve revealed that the fluorescence intensity at 597 nm increased linearly with increasing concentrations of Cu^{2+} between 0.10 and 10.0 μM. Mechanistic studies suggested that the probe opened its spiro-ring by a Cu^{2+}-induced transformation of the cyclic thiosemicarbazide moiety to an isothiocyanate group to afford **59**.

Replacement of bridge oxygen atom in the xanthene ring at position 10

Through substitution of the bridge oxygen atom by a silicon atom in the rhodamine framework (Fig. 56), a new strong fluorescent silaanthracene dye **60** has been developed by Xiao and co-workers which results in a 90 nm red shift in absorption relative to its conventional counterpart, **61**, and exhibits a high molar extinction coefficient.[72] This is the first case where the silicon atom is adopted as the functional element into the key position of a conventional excellent dye to successfully modulate the spectral properties. The electrochemical studies indicate that the smaller energy gap of **60** results from both energy decrease in LUMO and energy increase in HOMO.

Based on the Si-rhodamine framework combined with a spiro-thioether scaffold, a far-red to near-infrared (NIR) fluorescent probe (Fig. 57), **62**, was designed and synthesized by Nagano's group for sensitive and selective detection of HOCl in real time.[73] When **62** reacted with HOCl, a large and immediate increase in fluorescence intensity was observed (Abs_{max}/Em_{max} = 652/670 nm, $\varepsilon = 1.2 \times 10^5$, $\Phi_{fl} = 0.31$, in PBS), owing to the formation of highly fluorescent **64** and the fluorescence intensity change was linearly

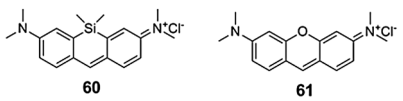

Fig. 56 Rhodamine-derivative with bridge silicon atom.

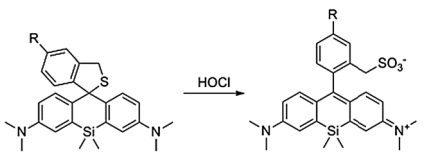

Fig. 57 Sensing of HClO through an oxidative opening the spiro-thioether ring in Si-rhodamine framework.

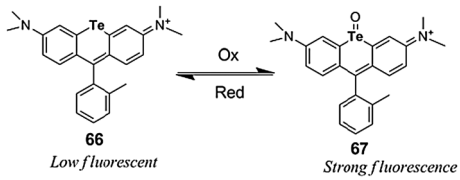

Fig. 58 Reversible Te-bridged rhodamine-based probe for reactive oxygen species.

related to the concentration of HOCl. In contrast, other ROS produced almost no fluorescence increase. **62** and its oxidized product **64** have excellent properties, including pH-independence of fluorescence, high resistance to autoxidation and photobleaching, and good tissue penetration of far-red to NIR fluorescence emission. With **62**, they conducted real-time imaging of phagocytosis by means of fluorescence microscopy, and, with the more hydrophilic derivative **63**, noninvasive *in vivo* imaging of HOCl generation in a mouse peritonitis model was achieved. The probes are expected to be useful tools for investigation of the wide range of biological functions of HOCl.

As demonstrated above, the spectroscopic properties of rhodamine dyes were proved to be tuned by replacement of the bridge oxygen atom in the xanthene moiety with other element atoms. As a consequence, an interesting tellurium–rhodamine was also reported by Nagano and co-workers (Fig. 58).[74] The O atom at the bridge position was replaced with Te atom to afford a Te-bridged rhodamine, **66**, which exhibited a relatively long absorption spectral band centered at 600 nm and nonfluorescent due to the heavy-atom effect of the Te atom. **66** was found to be selectively oxidized by reactive oxygen species (ROS) and the oxidized form, **67**, exhibited a large red shift in the absorption spectra at 669 nm compared with **66** at 600 nm and showed strong fluorescence at 690 nm with a fluorescence yield of 0.18, which is resulted from the weakened heavy-atom effect of the Te atom by the binding of an oxygen atom on it. Furthermore, **67** was found to be quickly converted to **66** in the presence of GSH, suggesting **66** could be used as a reversible probe for ROS. The system was confirmed to work in live HL-60 cells.

Chemosensors derived from the phenyl ring at positions 4′ and/or 5′

By bounding the macrocyclic polyamine directly to the fluorescein skeleton (Fig. 59), Nagano and co-workers developed the

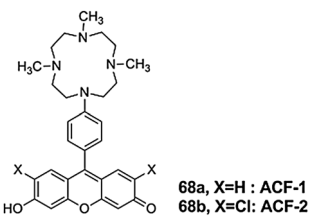

Fig. 59 Macrocyclic polyamine-based turn-on type fluorescent probes for Zn^{2+}.

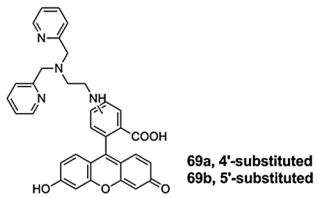

Fig. 60 *N*,*N*-bis (2-pyridylmethyl)ethylenediamine-based turn-on type fluorescent probes for Zn^{2+}.

fluorescent probes, **68a** and **68b**, for Zn^{2+}, in which the fluorescence is quenched due to photoinduced electron transfer (PET) by attaching an amino group to the phthalic ring of fluorescein, and the fluorophore aniline nitrogen results in lower pK_a values and consequently the **ACF**-Zn^{2+} complex can fluoresce at a physiological pH (pH 7.5, 100 mM HEPES buffer).[75] The detection limits of both **68a** and **68b** are *ca.* 500 nM of Zn^{2+} under pH 7.5, and these two probes also show high selectivity to Zn^{2+} over other various cations.

A couple of fluorescent Zn^{2+} sensor molecules (Fig. 60), **69**, which possess the characteristics of improved selectivity and faster complex formation was developed by Nagano and co-workers.[76] When Zn^{2+} is added to **69**, the four nitrogen atoms of the acceptor, *N*,*N*-bis (2-pyridylmethyl) ethylenediamine, form a four-coordinate complex, which hampers the photoinduced electron transfer (PET) process from the amino group to the xanthene fluorophore, resulting in strong fluorescence augmentation. The fluorescence intensity was increased by 17-fold and 51-fold for **69a** and **69b**, respectively, and **69a** is the first Zn^{2+} sensor molecule that can distinguish Cd^{2+} from Zn^{2+}. The detection limit of **69** is in the sub-nM range, which affords sufficient sensitivity for application in mammalian cells.

Gee and co-workers also reported the synthesis and fluorescence properties of an outstanding tetraanionic Zn^{2+}-selective fluorescent probe (Fig. 61), **70**, and its application in the imaging of zinc secretion from pancreatic β-cells.[77] The new dye had shown its high signal-to-noise ratio, more fluorescence enhancement, and good selectivity for zinc over calcium. Besides, it had stable fluorescence from pH 6 to 9.

A water-soluble fluorescent chemosensor (Fig. 62), **71**, was reported by Chang and co-workers to screen mercury levels in

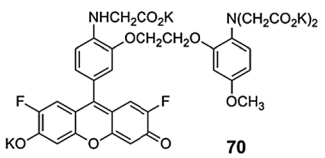

Fig. 61 Fluorescein-based tetraanionic Zn^{2+}-selective probe.

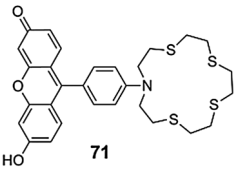

Fig. 62 Fluorescein-based probe bearing a thioether-rich crown receptor for Hg^{2+}.

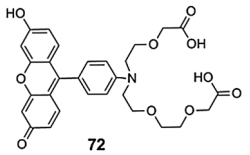

Fig. 63 Fluorescein-based probe **72** for Pb^{2+}.

fish.[78] **71** is virtually nonfluorescent ($\Phi < 0.001$), indicative of efficient photoinduced electron transfer (PET) quenching of the fluorophore by the azathiacrown receptor. Upon addition of Hg^{2+} under simulated physiological conditions (20 mM HEPES buffer, pH 7), the fluorescence intensity of **71** increases by over 170-fold with a 60 nM detection limit for aqueous Hg^{2+}. **71** exhibits excellent selectivity for Hg^{2+} over competing environmentally relevant metal ions. Furthermore, experiments with fish show that **71** is capable of reliably detecting mercury levels in fish over a range of 0.1 to 8 ppm, which is well within the safe edible limit.

Chang and co-workers further presented the synthesis and properties of chemosensor **72** (Fig. 63), a new turn-on fluorescent sensor for selective detection of Pb^{2+} in water and in living cells.[79] **72** features visible wavelength excitation and emission profiles and a *ca.* 18-fold fluorescence enhancement upon Pb^{2+} binding. This fluorescein-based reagent displays a selective turn-on response for Pb^{2+} over competing metal ions such as Li^+, Na^+, K^+, Mg^{2+}, Ca^{2+}, Mn^{2+}, Fe^{2+}, Co^{2+}, Ni^{2+}, Cu^{2+}, Cu^+, Zn^{2+}, Cd^{2+}, Hg^{2+} in water, with sensitivity to EPA limits of lead poisoning. Moreover, confocal microscopy experiments establish that **72** can monitor changes in Pb^{2+} levels within living mammalian cells.

Suzuki and co-workers devised three novel Mg^{2+} fluorescent probes **73a**, **73b** and **73c**, which were characterized by having a strong PET-type fluorescence enhancement upon magnesium binding (Fig. 64).[80] The compounds of this series feature a charged β-diketone as a binding site specific for Mg^{2+} and a fluorescein residue as the fluorophore that can be excited with an Ar^+ laser, commonly used in confocal scanning microscopy. The two fluorescent probes **73a** and **73b** showed suitable dissociation constants (K_d = 2 mM) and nearly a 10-fold fluorescence enhancement over the intracellular magnesium ion concentration range (0.1–6 mM), allowing high-contrast, sensitive, and selective Mg^{2+} measurements. By cell loading in the form of the acetoxymethyl derivative of **73b**, the probe can easily be applied to intracellular imaging.

Since Glutathione S-transferase (GST) is of clinical interest, based on the donor-excited photoinduced electron transfer (d-PET) process from the excited fluorophore to the electron-deficient benzene moiety, dinitrobenzanilide, Nagano and co-workers reported

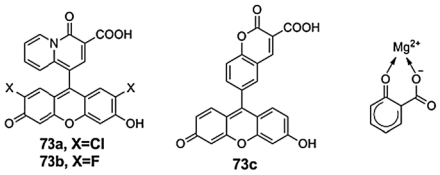

Fig. 64 Series of turn-on fluorescein-based probes for Mg^{2+} and their plausible binding mode.

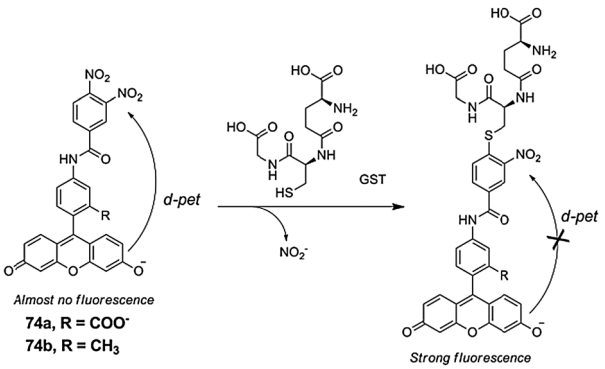

Fig. 65 Reaction of probes **74** with GSH in the presence of GST.

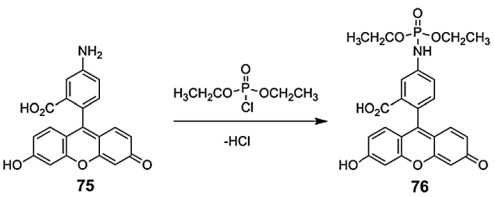

Fig. 66 Sensing of diethyl chlorophosphate by formation of phosphoramide.

the excellent fluorescent chemodosimeter **74a** for GST with an "Off–On" fluorescence-switching behavior by the replacement of a nitro group with GSH followed by a 34-fold increase in the quantum efficacy (Fig. 65).[81] The chemodosimeter is highly sensitive and suitable for high-throughput screening. Furthermore, the membrane permeable derivative **74b** was synthesized, which was used for visualizing high GST activity in the nucleus of HuCCT1 cells.

Walt and co-workers described the preparation and application of microbeads loaded with **75** that exhibited a turn-on fluorescence response within seconds of exposure to diethyl chlorophosphate (DCP) vapor (Fig. 66).[82] **75** is quenched relative to its acyl derivative because the lone pair nitrogen of the amine group quenches the fluorescence *via* photoinduced electron transfer (PET). Upon reaction with a phosphoryl group, the amino group's lone pair is less available and increased fluorescence is observed for the conversion of **75** into a phosphoramide product, **76.**

Nagano and co-workers designed **77a** (DAF-2) as a novel fluorescent indicator for NO in neutral pH buffers (Fig. 67).[83]

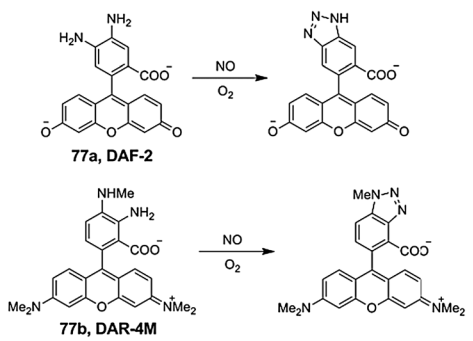

Fig. 67 NO probes based on aromatic vicinal diamines **77**.

The fluorescence chemical transformation of DAF-2 is based on the reactivity of the aromatic vicinal diamines with NO in the presence of dioxygen. The N-nitrosation of DAF-2, yielding the highly green-fluorescent triazole form, offers the advantages of specificity, sensitivity, and a simple protocol for the direct detection of NO (detection limit 5 nM). Furthermore, membrane-permeable DAF-2 diacetate (DAF-2 DA) can be used for real-time bioimaging of NO with fine temporal and spatial resolution. However, the fluorescence of the fluorescein-based chromophore is pH-sensitive and overlaps the autofluorescence of cells. To obtain higher photostability, longer excitation wavelength, and applicability over a wider pH range, they further developed a fluorescent indicator for NO based on the rhodamine chromophore, **77b** (DAR-4M), which can be excited with 550 nm light.[84] The fluorescence quantum yield of the product after reaction with NO is 840 times higher than that of DAR-4M. The detection limit of NO was 7 nM, and the fluorescence showed no pH dependency above pH 4. Its acetoxymethyl acetate, a membrane-permeable derivative, DAR-4M AM was successfully applied to practical bioimaging of NO produced in bovine aortic endothelial cells with almost no autofluorescence of the cells due to the longer wavelength excitation.

Based on the fact that HS^- is known to react with copper ions to form CuS species, the azamacrocyclic–copper(II) ion complex chemistry was employed by Nagano and co-workers to design a Cu^{2+} complex as a novel fluorescent probe (Fig. 68), **78**, for H_2S, in which the fluorescein-based ligand displays a fluorescence quenching effect with Cu^{2+} and the addition of HS^- to this solution induced "Off–On" type fluorescence enhancement.[85] **78** can sensitively detect H_2S in aqueous solution (30 mM HEPES buffer, pH 7.4 at 37 °C) with high selectivity over biothiols, inorganic sulfur compounds, ROS, and RNS. In addition, diacetylated **78** was confirmed to be membrane-permeable and could be used for real-time fluorescence imaging of intracellular H_2S in live cells.

Utilizing a benzil chemistry as well as the donor-excited photoinduced electron transfer (d-PET) process to control the fluorescence, Nagano and co-workers designed a novel fluorescent probe, **79**, for hydrogen peroxide (Fig. 69).[86] **79** did not show any fluorescence enhancement in response to superoxide ($O_2^{\bullet-}$), hydroxyl radical ($^{\bullet}OH$), hypochlorite (ClO^-), nitric oxide (NO), or singlet oxygen ($^1O_2$) and only small fluorescence enhancements were observed with peroxynitrite ($ONOO^-$) and *tert*-butyl hydroperoxide (TBHP). It afforded the highly sensitive detection of hydrogen peroxide owing to its extremely low background fluorescence with a good reaction rate and high specificity, and the enhancement of fluorescence intensity after reaction with hydrogen peroxide was as high as 150-fold in 0.1 M sodium phosphate buffer at pH 7.4. Further, **79** was employed for application in bioimaging of hydrogen peroxide.

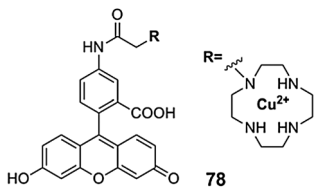

Fig. 68 Turn-on fluorescein-based ensemble probe for H_2S by formation of CuS species.

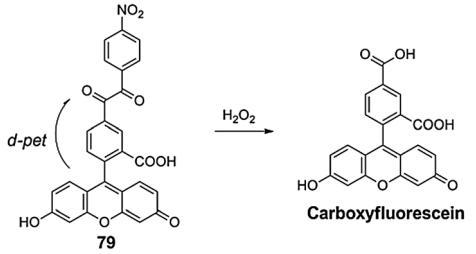

Fig. 69 Benzil-based chemodosimeter for H_2O_2.

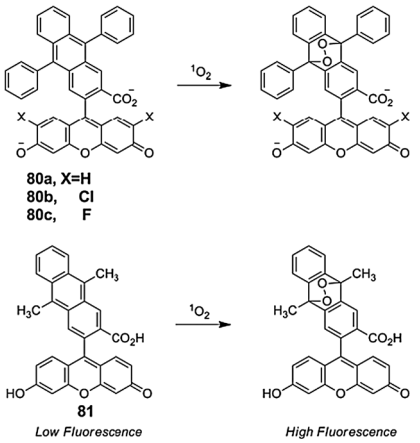

Fig. 70 Sensing of singlet oxygen by formation of *endo*-peroxides of anthracene derivatives.

Nagano and co-workers developed turn-on probes (Fig. 70), **80a–c** for singlet oxygen, based on the cycloaddition to the anthracene moiety.[87] **80a–c** themselves are almost nonfluorescent, however, their *endo*-peroxide products are highly fluorescent. These probes do not respond to H_2O_2, superoxide, and nitric oxide. Since **80a–c** have some limitations in application to biological systems, especially with regard to their sensitivity. In order to solve those problems, thereafter, they developed a novel fluorescent probe, **81**, for $^1O_2$.[88] The fluorescence properties of **81** are controlled by a photoinduced electron transfer (PET) process from the benzoic acid moiety to the xanthene ring, and **81** has a 31-fold faster rate constant and is 53-fold more sensitive than **80a.** These results indicate that **81** is an excellent fluorescent probe for $^1O_2$, and it should be widely useful in biological systems.

Conclusion

Fluorescent sensors have consistently demonstrated their potential in biological and environmental applications. As both excellent fluorophore and chromophore probes, the fluorescein and rhodamine fluorochromes have still attracted considerable interest from chemists on account of their preferable practical

properties, such as good water solubility, nontoxicity, and the ability to function at physiological pH. This feature article provides insight into how the modification of the sites in the skeleton of fluorescein and rhodamine dyes can be utilized, and in due course, into what a wide range of chemosensors have been developed and have proven to be good sensing systems. The selective examples in this article clearly indicated that these types of modifications have advantages of the diversity in the practice of molecular design, and consequently, the fluorescence sensing of a wide range of analytes, including metal ions, anions, neutral molecules as well as biologically related oxidative- and reductive-species can be achieved. On the other hand, some unique scaffolds may originate from the modification in the skeleton of rhodamine or fluorescein dyes, for example, Si-substituted xanthene analogue, which exhibits remarkable red shift in fluorescence emission compared to its O-substituted counterpart, may possess great potential in fabrication of series of far-red fluorescent probes for sensing purpose, or in biological applications, especially in the bio-imaging field. For another example, the latest report of modification in carboxylic group results in a novel spiro-form of the rhodamine scaffold that contains a six-membered reactive ring, which may also provide a new basis for the design of a series of interesting spiro-rhodamine-based fluorescent chemosensors. Based on the versatile means of modification in xanthene-based fluorophore, we can envision that there still present ample opportunities for designing efficient and novel fluorescent probes in this field.

This work was financially supported by the National Natural Science Foundation of China (No. 20675067, No. 20835005 and No. 81071202), which is gratefully acknowledged.

Notes and references

1 E. Noelting and K. Dziewonsky, *Ber. Dtsch. Chem. Ges.*, 1905, **38**, 3516.
2 A. von Bayer, *Chem. Ber.*, 1871, **5**, 255.
3 H. N. Kim, M. H. Lee, H. J. Kim, J. S. Kim and J. Yoon, *Chem. Soc. Rev.*, 2008, **37**, 1465–1472.
4 M. Beija, C. A. M. Afonso and J. M. G. Martinho, *Chem. Soc. Rev.*, 2009, **38**, 2410–2433.
5 D. T. Quang and J. S. Kim, *Chem. Rev.*, 2010, **110**, 6280–6301.
6 M. E. Jun, B. Roy and K. H. Ahn, *Chem. Commun.*, 2011, **47**, 7583–7601.
7 X. Q. Chen, T. Pradhan, F. Wang, J. S. Kim and J. Yoon, *Chem. Rev.*, 2012, **112**, 1910–1956.
8 Y. M. Yang, Q. Zhao, W. Feng and F. Y. Li, *Chem. Rev*, 2012, DOI: dx.doi.org/10.1021/cr2004103.
9 K. Setsukinai, Y. Urano, K. Kakinuma, H. J. Majima and T. Nagano, *J. Biol. Chem.*, 2003, **278**, 3170–3175.
10 H. Maeda, K. Yamamoto, Y. Nomura, I. Kohno, L. Hafsi, N. Ueda, S. Yoshida, M. Fukuda, Y. Fukuyasu, Y. Yamauchi and N. Itoh, *J. Am. Chem. Soc.*, 2005, **127**, 68.
11 K. H. Xu, X. Liu, B. Tang, G. W. Yang, Y. Yang and L. G. An, *Chem.–Eur. J.*, 2007, **13**, 1411–1416.
12 H. Maeda, Y. Fukuyasu, S. Yoshida, M. Fukuda, K. Saeki, H. Matsuno, Y. Yamauchi, K. Yoshida, K. Hirata and K. Miyamoto, *Angew. Chem., Int. Ed.*, 2004, **43**, 2389.
13 D. Yang, H. L. Wang, Z. N. Sun, N. W. Chung and J. G. Shen, *J. Am. Chem. Soc.*, 2006, **128**, 6004.
14 Y. Zhou, J. Y. Li, K. H. Chu, K. Liu, C. Yao and J. Y. Li, *Chem. Commun.*, 2012, **48**, 4677.
15 A. L. Garner, C. M. St Croix, B. R. Pitt, G. D. Leikauf, S. Ando and K. Koide, *Nat. Chem.*, 2009, **1**, 316.
16 M. G. Choi, S. Cha, J. E. Park, H. Lee, H. L. Jeon and S. K. Chang, *Org. Lett.*, 2010, **12**, 1468.
17 H. Matsuno, M. Ushida, H. Maeda, K. Katayama, K. Saeki and N. Itoh, *Angew. Chem.*, 2005, **44**, 2922.
18 H. Maeda, K. Katayama, H. Matsuno and T. Uno, *Angew. Chem., Int. Ed.*, 2006, **45**, 1810.
19 B. Tang, Y. Xing, P. Li, N. Zhang, F. Yu and G. Yang, *J. Am. Chem. Soc.*, 2007, **129**, 11666.
20 B. Tang, L. Yin, X. Wang, Z. Chen, L. Tong and K. Xu, *Chem. Commun.*, 2009, 5293.
21 M. M. Pires and J. Chmielewski, *Org. Lett.*, 2008, **10**, 837.
22 X. Yang, Y. Guo and R. M. Strongin, *Org. Biomol. Chem.*, 2012, **10**, 2739.
23 M. Santra, D. Ryu, A. Chatterjee, S.-K. Ko, I. Shin and K. H. Ahn, *Chem. Commun.*, 2009, 2115.
24 F. Song, A. L. Garner and K. Koide, *J. Am. Chem. Soc.*, 2007, **129**, 12354.
25 A. L. Garner and K. Koide, *J. Am. Chem. Soc.*, 2008, **130**, 16472.
26 M. Santra, S. K. Ko, I. Shin and K. H. Ahn, *Chem. Commun.*, 2010, **46**, 3964.
27 M. Taki, S. Iyoshi, A. Ojida, I. Hamachi and Y. Yamamoto, *J. Am. Chem. Soc.*, 2010, **132**, 5938.
28 H. Y. Au-Yeung, E. J. New and C. J. Chang, *Chem. Commun.*, 2012, **48**, 5268–5270.
29 C. Liu, J. Pan, S. Li, Y. Zhao, L. Y. Wu, C. E. Berkman, A. R. Whorton and M. Xian, *Angew. Chem., Int. Ed.*, 2011, **50**, 10327.
30 C. Liu, B. Peng, S. Li, C. M. Park, A. R. Whorton and M. Xian, *Org. Lett.*, 2012, **14**, 2184.
31 G. A. Smith, J. C. Metcalfe and S. D. Clarke, *J. Chem. Soc. Perkin Trans. 2*, 1993, 1195.
32 E. Tomat and S. J. Lippard, *Inorg. Chem.*, 2010, **49**, 9113–9115.
33 X. Lv, J. Liu, Y. Liu, Y. Zhao, M. Chen, P. Wang and W. Guo, *Sens. Actuators, B*, 2011, **158**, 405.
34 E. M. Nolan and S. J. Lippard, *J. Am. Chem. Soc.*, 2003, **125**, 14270.
35 M. G. Choi, D. H. Ryu, H. L. Jeon, S. Cha, J. Cho, H. H. Joo, K. S. Hong, C. Lee, S. Ahn and S. K. Chang, *Org. Lett.*, 2008, **10**, 3717.
36 S. C. Burdette, G. K. Walkup, B. Spingler, R. Y. Tsien and S. J. Lippard, *J. Am. Chem. Soc.*, 2001, **123**, 7831.
37 S. C. Burdette, C. J. Frederickson, W. Bu and S. J. Lippard, *J. Am. Chem. Soc.*, 2003, **125**, 1778.
38 X. Zhang, D. Hayes, S. J. Smith, S. Friedle and S. J. Lippard, *J. Am. Chem. Soc.*, 2008, **130**, 15788.
39 E. M. Nolan, J. Jaworski, K. I. Okamoto, Y. Hayashi, M. Sheng and S. J. Lippard, *J. Am. Chem. Soc.*, 2005, **127**, 16812.
40 W. Liu, L. Xu, R. Sheng, P. Wang, H. Li and S. Wu, *Org. Lett.*, 2007, **9**, 3829.
41 K. M. K. Swamy, H. N. Kim, J. H. Soh, Y. Kim, S. Kim and J. Yoon, *Chem. Commun.*, 2009, 1234.
42 W. Wang, O. Rusin, X. Xu, K. K. Kim, J. O. Escobedo, S. O. Fakayode, K. A. Fletcher, M. Lowry, C. M. Schowalter, C. M. Lawrence, F. R. Fronczek, I. M. Warner and R. M. Strongin, *J. Am. Chem. Soc.*, 2005, **127**, 15949.
43 X. Q. Chen, S. K. Ko, M. J. Kim, I. Shin and J. Yoon, *Chem. Commun.*, 2010, **46**, 2751.
44 S. K. Kwon, S. Kou, H. N. Kim, X. Chen, H. Hwang, S. W. Nam, S. H. Kim, K. M. K. Swamy, S. Park and J. Yoon, *Tetrahedron Lett.*, 2008, **49**, 4102.
45 S. Y. Chung, S. W. Nam, J. Lim, S. Park and J. Yoon, *Chem. Commun.*, 2009, 2866.
46 X. Lv, J. Liu, Y. Liu, Y. Zhao, M. Chen, P. Wang and W. Guo, *Org. Biomol. Chem.*, 2011, **9**, 4954.
47 K. M. K. Swamy, Y. J. Lee, H. N. Lee, J. Chun, Y. Kim, S. J. Kim and J. Yoon, *J. Org. Chem.*, 2006, **71**, 8626.
48 M. H. Lim, B. A. Wong, W. H. Pitcock Jr., D. Mokshagundam, M. H. Baik and S. J. Lippard, *J. Am. Chem. Soc.*, 2006, **128**, 14364.
49 D. Song, J. M. Lim, S. Cho, S. J. Park, J. Cho, D. Kang, S. G. Rhee, Y. You and W. Nam, *Chem. Commun.*, 2012, **48**, 5449.
50 X. Cheng, H. Jia, T. Long, J. Feng, J. Qin and Z. Li, *Chem. Commun.*, 2011, **47**, 11978.
51 M. C. Y. Chang, A. Pralle, E. Y. Isacoff and C. J. Chang, *J. Am. Chem. Soc.*, 2004, **126**, 15392.
52 B. C. Dickinson and C. J. Chang, *J. Am. Chem. Soc.*, 2008, **130**, 9638–9639.

53 A. E. Albers, V. S. Okreglak and C. J. Chang, *J. Am. Chem. Soc.*, 2006, **128**, 9640.
54 A. R. Lippert, E. J. New and C. J. Chang, *J. Am. Chem. Soc.*, 2011, **133**, 10078.
55 Y. Koide, Y. Urano, S. Kenmoku, H. Kojima and T. Nagano, *J. Am. Chem. Soc.*, 2007, **129**, 10324.
56 S. Kenmoku, Y. Urano, H. Kojima and T. Nagano, *J. Am. Chem. Soc.*, 2007, **129**, 7313.
57 Q. A. Best, R. Xu, M. E. McCarroll, L. Wang and D. J. Dyer, *Org. Lett.*, 2010, **12**, 3219.
58 X. Wu, Z. Wu and S. Han, *Chem. Commun.*, 2011, **47**, 11468.
59 X. Wu, Z. Wu, Y. Yang and S. Han, *Chem. Commun.*, 2012, **48**, 1895.
60 W. Lin, L. Long, B. Chen, W. Tan and W. Gao, *Chem. Commun.*, 2010, **46**, 1311.
61 S. Wen and H. M. Ma, *Chem. Commun.*, 2008, **16**, 1856.
62 X. Q. Zhan, Z. H. Qian, H. Zheng, B. Y. Su, Z. Lan and J. G. Xu, *Chem. Commun.*, 2008, **16**, 1859.
63 X. Q. Chen, S. W. Nam, M. J. Jou, Y. Kim, S. J. Kim, S. Park and J. Yoon, *Org. Lett.*, 2008, **10**, 5235.
64 X. Q. Zhan, J. H. Yan, H. Zheng and J. G. Xu, *Sens. Actuators, B*, 2010, **150**, 774–780.
65 X. Chen, K. A. Lee, E. M. Ha, K. M. Lee, Y. Y. Seo, H. K. Choi, H. N. Kim, M. J. Kim, C. S. Cho, S. Y. Lee, W. J. Lee and J. Yoon, *Chem. Commun.*, 2011, **47**, 4373–4375.
66 W. Shi, S. Sun, X. H. Li and H. M. Ma, *Inorg. Chem.*, 2010, **49**, 1206–1210.
67 X. Chen, K. H. Baek, Y. Kim, S. J. Kim, I. Shin and J. Yoon, *Tetrahedron*, 2010, **66**, 4016–4021.
68 C. Sun, W. Shi, Y. Song, W. Chen and H. M. Ma, *Chem. Commun.*, 2011, **47**, 8638.
69 L. Long, W. Lin, B. Chen, W. Gao and L. Yuan, *Chem. Commun.*, 2011, **47**, 893.
70 H. Zheng, Z. H. Qian, L. Xu, F. F. Yuan, L. D. Lan and J. G. Xu, *Org. Lett.*, 2006, **8**, 859–861.
71 C. Wu, Q. N. Bian, B. G. Zhang, X. Cai, S. D. Zhang, H. Zheng, S. Y. Yang and Y. B. Jiang, *Org. Lett.*, 2012, **14**, 4198.
72 M. Fu, Y. Xiao, X. Qian, D. Zhao and Y. Xu, *Chem. Commun.*, 2008, 1780.
73 Y. Koide, Y. Urano, K. Hanaoka, T. Terai and T. Nagano, *J. Am. Chem. Soc.*, 2011, **133**, 5680.
74 Y. Koide, M. Kawaguchi, Y. Urano, K. Hanaoka, T. Komatsu, M. Abo, T. Terai and T. Nagano, *Chem. Commun.*, 2011, **48**, 3091–3093.
75 T. Hirano, K. Kikuchi, Y. Urano, T. Higuchi and T. Nagano, *Angew. Chem., Int. Ed.*, 2000, **39**, 1052.
76 T. Hirano, K. Kikuchi, Y. Urano, T. Higuchi and T. Nagano, *J. Am. Chem. Soc.*, 2000, **122**, 12399.
77 K. R. Gee, Z. L. Zhou, W. J. Qian and R. Kennedy, *J. Am. Chem. Soc.*, 2002, **124**, 776.
78 S. Yoon, A. E. Albers, A. P. Wong and C. J. Chang, *J. Am. Chem. Soc.*, 2005, **127**, 16030.
79 Q. He, E. W. Miller, A. P. Wong and C. J. Chang, *J. Am. Chem. Soc.*, 2006, **128**, 9316.
80 H. Komatsu, N. Iwasawa, D. Citterio, Y. Suzuki, T. Kubota, K. Tokuno, Y. Kitamura, K. Oka and K. Suzuki, *J. Am. Chem. Soc.*, 2004, **126**, 16353.
81 Y. Fujikawa, Y. Urano, T. Komatsu, K. Hanaoka, H. Kojima, T. Terai, H. Inoue and T. Nagano, *J. Am. Chem. Soc.*, 2008, **130**, 14533.
82 S. Bencic-Nagale, T. Sternfeld and D. R. Walt, *J. Am. Chem. Soc.*, 2006, **128**, 5041.
83 H. Kojima, N. Nakatsubo, K. Kikuchi, S. Kawahara, Y. Kirino, H. Nagoshi, Y. Hirata and T. Nagano, *Anal. Chem.*, 1998, **70**, 2446.
84 H. Kojima, M. Hirotani, N. Nakatsubo, K. Kikuchi, Y. Urano, T. Higuchi, Y. Hirata and T. Nagano, *Anal. Chem.*, 2001, **73**, 1967.
85 K. Sasakura, K. Hanaoka, N. Shibuya, Y. Mikami, Y. Kimura, T. Komatsu, T. Ueno, T. Terai, H. Kimura and T. Nagano, *J. Am. Chem. Soc.*, 2011, **133**, 18003.
86 M. Abo, Y. Urano, K. Hanaoka, T. Terai, T. Komatsu and T. Nagano, *J. Am. Chem. Soc.*, 2011, **133**, 10629.
87 N. Umezawa, K. Tanaka, Y. Urano, K. Kikuchi, T. Higuchi and T. Nagano, *Angew. Chem., Int. Ed.*, 1999, **38**, 2899.
88 K. Tanaka, T. Miura, N. Umezawa, Y. Urano, K. Kikuchi, T. Higuchi and T. Nagano, *J. Am. Chem. Soc.*, 2001, **123**, 2530.